C 1

SOME NEW APPROACHES TO GRAVITY MODELLING

by

WILLIAM ROBERT GREEN

B.A.Sc., University of British Columbia, 1970

A THESIS SUBMITTED IN PARTIAL FULFILMENT OF

THE REQUIREMENTS FOR THE DEGREE OF

MASTER OF SCIENCE

in the Department

of

GEOPHYSICS

We accept this thesis as conforming to the

required standard

THE UNIVERSITY OF BRITISH COLUMBIA

May, 1973

In presenting this thesis in partial fulfilment of the requirements for

an advanced degree at the University of British Columbia, I agree that

the Library shall make it freely available for reference and study.

I further agree that permission for extensive copying of this thesis

for scholarly purposes may be granted by the Head of my Department or

by his representatives. It is understood that copying or publication

of this thesis for financial gain shall not be allowed without my

written permission.

Department of Geophysics

The University of British Columbia
Vancouver 8, Canada

Date May 28, 1973

ABSTRACT

Geophysical inversion methods are most effective when applied to linear functionals; it is therefore advantageous to employ linear models for geophysical data. A two-dimensional linear model consisting of many horizontal prisms has been developed for interpretation of gravity profiles. A Backus-Gilbert inversion which finds the acceptable model "nearest" to an initial estimate can be rapidly computed; iterative application of the technique allows a single-density model to be developed at modest expense of computer time. Gravity data from the Guichon Creek batholith were inverted as a test of the method, with results comparable to a standard polygon model.

The entropy of these linear models is a useful property which can be minimized to find an optimum "structured" or "compact" model. Since a numerical optimization is used, computations become prohibitively long for any large number of parameters. Several simple models have been found by minimizing the entropy of an intial model under the constraints imposed by a known gravity profile. Similar results can be obtained by using a simpler objective function. It is also possible to maximize model entropy; this procedure tends to evenly distribute the anomalous mass beneath the profile, while minimum entropy tries to concentrate mass in as few prisms of the model as possible.

TABLE OF CONTENTS

LIST OF TABLES

LIST OF FIGURES

ACKNOWLEDGEMENTS

CHAPTER 1

Introduction To Gravity Modelling

There are three major steps necessary to obtain useful information

from geophysical explorations; data acquisition, analysis, and interpretation.

Data must first be recorded in the field with sufficient accuracy to allow

drawing geological conclusions. Secondly, the data must be analyzed and

put into a form which enable them to be related to properties of the explo-

ration objective. Finally, by applying theoretical knowledge of the rela-

tionships between physical properties of the earth and the type of data under

consideration, one can estimate those physical properties in the explored

region. This thesis will consider some new variants of this third stage in

the treatment of gravity data.

Before any geophysical data can be used to estimate the physical

parameters of the earth, it is necessary to solve the "direct problem" for

the particular type of data. The direct (or forward) problem consists of

predicting values of a geophysical function from known parameters of the

earth. For example, if free oscillation data are to yield information

about the earth's density, the relationship between the periods of the oscil-

lations and a known density function must be known; i.e. one must be able

to accurately predict the oscillation periods for a hypothetical earth of

known density. Fortunately the direct problem of finding the gravitational

attraction of a given density distribution (e.g. a body of known shape,

location, and density) can be solved using potential theory (MacMillan 1930).

If the forward problem can be solved, it may be possible to find

solutions to the "inverse problem", which attempts to find physical para-
meters of the earth from observed values of certain geophysical functions.
Geophysical inversion frequently is a problem in modelling: one seeks
parameters for a model whose properties correspond to observations of the
real earth, by using the solution to the direct problem for the model para-
meters and type of data available. The parameters may be determined in two
ways: by an analytic method based on the functional relationship of the
parameters to the data; or by a trial-and-error process in which an inter-
preter adjusts model parameters in an attempt to improve the fit to the
data (in this case, he is continually solving the direct problem, rather
than finding a formal solution to the inverse problem). A simple example
of inversion is refraction seismology, where the objectives are the velocities
and thicknesses of crustal layers which produce the observed travel times
at the surface.

In many cases, inversion is a subjective process without exact
solution. To begin with, the infinite detail of the real earth cannot be
uniquely determined from the finite number of observations available. It
may also be true that several models can satisfy the same set of data, if
those data are not in themselves sufficient to determine a unique model.
This is true of gravity data, as it is well known that many quite different
density distributions may produce identical gravity anomalies (Skeels, 1947).
The non-uniqueness of inverse problems has been treated in different ways.
Many techniques impose enough constraints on the model being sought to ensure
that it is unique. A similar, but conceptually simpler, viewpoint is to
seek particular members of the set of models which satisfy the data, usually

by optimizing some property of the model, for example, finding the "nearest" acceptable model to a specified initial model which does not satisfy the data.

Several different types of models may be used with the same data, and the inversion procedure will naturally depend on the type of parameters being used. For example, the parameters of a gravity model might be the external shape and constant density of an anomalous body, or perhaps the density at various points in a given subsurface region. In some problems, the speed and efficiency of the inversion may be improved by defining a new type of model whose parameters are more simply related to the observed data. Linear models are often preferable, since they obviate the need for iterative procedures required in fitting non-linear models to the data. By a linear model, we mean a model whose parameters are linearly related to the observed geophysical data.

The inverse problem in gravity exploration has usually been approached by considering restricted classes of models with only a few parameters, and adjusting an initial model to find a "best-fit" solution; this has generally meant non-linear models and hence iterative methods. With the viewpoint of finding particular models in a large set, the linearity of the density-gravity relationship can be exploited to develop new modelling techniques. Before considering methods, a brief description of the objectives and requirements of the inversion process is in order.

Several types of anomalies may be found in the earth's gravity

field, by applying different corrections to the total field (e.g. free-air anomaly, Bouguer anomaly, isostatic anomaly: see Garland, 1965, Chapter 4); different interpretation methods can be developed for different types of anomalies. Modelling techniques for exploration data usually attempt to define a single subsurface formation to account for an isolated anomaly (Grant and West, 1965, p. 268, term this "quantitative interpretation"). The anomaly is defined by applying all necessary corrections to the raw data (e.g. latitude, free-air, Bouguer, terrain) to find the Bouguer anomaly (Grant and West, 1965, pp. 236-243), and then removing regional variations from the Bouguer gravity to locate isolated, local features. The anomaly should then be due solely to some isolated body whose density is different from the crustal average.

The separation of local anomalies from the regional field requires great care, since the shape of residual anomalies can be altered by the separation process (Skeels, 1967; Ulrych, 1968). Any analytic inversion procedure can only be successful if the anomalous gravity corresponds to a real feature of the earth, and is not even partly a result of a filtering process. If the regional separation is successful, a model can be formulated strictly in terms of the density contrast between an anomalous feature and the average crustal rocks. In this case, "density" can be taken to imply "density contrast."

The corrections applied in finding residual anomalies contain many uncertainties, and thus gravity models need not produce an exact fit to the observations (and usually cannot do so). For the purpose of studying

modelling techniques, we will assume that the anomalous gravity is exactly known, but frequently will accept a close fit rather than attempting to produce perfect agreement with the data. The remainder of the thesis is concerned with finding simple models from residual anomalies.

CHAPTER 2

Gravity Data And Inversion Techniques

2.1 Common Methods of Gravity Modelling

There are several ways to build models for the crustal structures

which produce gravity anomalies. A model could be formed by specifying:

the shape and position of a body of constant density; the location of a

number of simple bodies; the density (contrast) at various points in the

subsurface; or other parameters. The basis of the inversion process is to

establish the relationship between the model parameters and the surface

gravity (i.e. to solve the forward problem); and then apply the relationship

to compute a set of model parameters corresponding to the observed gravity.

The computational method will depend on the nature of the parameters, and

in some cases in merely trial and error adjustment to improve an initial

model.

Perhaps the most common methods of determining simple models from

gravity anomalies stem from the polygon methods of Talwani et al (1959) and

Talwani and Ewing (1960), developed to solve the direct problem for two and

three-dimensional features, respectively. The two-dimensional method assumes

the body to be an N-sided polygon of known, constant density; and uses the

positions of the vertices to compute the gravity effect of the body. By

specifying the locations of each vertex in an initial polygon, and comparing

the computed gravity to an observed surface gravity profile, one can make

iterative changes to the coordinates of each vertex until there is accept-

able agreement with the real data. A three-dimensional body can be modelled

with a series of horizontal lamina, each of polygonal outline. Again the gravity effect can be computed from the coordinates of each vertex and the given density, and iterative changes can be made to an initial model to produce good agreement with the measured gravity on the two-dimensional surface. Rather than using a trial and error basis for successive changes to the model, Corbato (1965) suggested a least-square error approach to improve a two-dimensional polygon, and thus accelerated convergence to the observed anomaly.

Another frequently used approach is to consider models consisting of many bodies of simple shape, for example, spheres or rectangular prisms. Tanner (1967) developed an iterative procedure to develop two-dimensional models consisting of constant density rectangular blocks. He assumed that the density, width, and depth to top of each block are known, so that the unknown parameters to be obtained are the depths to the bottom of each block. Dyrelius and Vogel (1972) also used this approach. Negi and Garde (1969) and Agarwal (1971) developed similar models, but allowed each vertical column to be subdivided into units of different density. Their methods were aimed at finding gravity models of sedimentary basins, where several layers of different density might be expected. Nagy (1966) used models consisting of three-dimensional prisms of various sizes and densities, and then used trial and error adjustment to improve the fit of an initial model to a gravity map. Cordell and Henderson (1968) found three-dimensional models made up of vertical prisms, using an automatic iterative method to solve for the depths of the prisms beneath a gridded two-dimensional surface.

Modelling is by no means the only way to usefully interpret gravity data. Many other approaches have been used, some of which are described by Garland (1965) and Grant and West (1965). One example is to examine the characteristics of potential fields in the spatial frequency domain (e.g. Odegard and Berg, 1965; Berezhnaya and Telepin, 1968). Another widely used method is downward continuation, which attempts to find the "topography" of a density interface (Grant and West, 1965). However, as this thesis is intended to give insight into modelling techniques, such other methods will not be discussed further.

2.2 Non-Uniqueness in Gravity Inversion

The greatest problem to be overcome in finding the source of a gravity anomaly is the non-uniqueness associated with potential field inversions; i.e. different bodies or crustal structures can produce the same gravity effect at the surface, and there is no way to distinguish which of the acceptable models corresponds to the real earth, from the gravity data alone. Skeels (1947) presented several examples of quite different formations which produce the same surface gravity. He also developed an analytic proof (using Green's theorem to integrate the vertical gravity effect around the body) to show that a layer of variable density can have the same gravity profile as a point mass at greater depth. Skeels noted that the ambiguity in interpretation can be considerably reduced if other geological or geophysical data are available.

In a further analysis of non-uniqueness, Roy (1962) studied situations in which a unique model could be developed; for example, if the

anomalous density is confined to a plane at known depth, there is only one density function which can produce a given gravity anomaly. He noted that this assumption is implicit in structural determination by downward continuation. Another unique class of models are those of constant density and known external shape; models of this type usually treat size, position, and orientation of the anomalous body as unknown parameters.

Al-Chalabi (1971) examined methods for finding models which provide unique solutions to the inverse problem. He discussed other (i.e. non-potential) sources of non-uniqueness, including incomplete knowledge of the anomaly; observational errors; and the use of simple models to describe the complicated real earth. He studied the results of modelling with polygons, using artificial gravity profiles from polygonal bodies. Unique solutions were possible if the model polygon had as many sides as the 'real' body; however, the uniqueness could be destroyed by inadequate profile length or other factors. If the model polygon had fewer sides than the real body, any solution would not be unique. Al-Chalabi's conclusions were: a satisfactory solution can be obtained by specifying only one model parameter, provided none of the factors contributing to ambiguity are too great; and, in cases where there are strong sources of ambiguity, it is desirable to produce a number of solutions by examining intervals in the parameter 'hyperspace' corresponding to acceptable agreement with the observed anomaly.

Most techniques for inverting gravity data avoid the problem of non-uniqueness by using restricted classes of models; solving for a very

limited number of unknown parameters may ensure that there is only one

model of that type which acceptably fits the data. The usual method is to

alter chosen parameters of an initial model to obtain agreement with the

observed gravity, and thus the final model may largely depend on the nature

of the initial model. In such methods, the "uniqueness" of the solution

may lie in being the acceptable model which most closely resembles the

initial estimate. It is possible that an inverse method thought to be

unique is not; for example, Parker (1973) found that the standard models

for magnetization of the oceanic crust (which are very similar to gravity

modelling using a constant thickness layer), do not provide a unique

inverse for the magnetic anomalies observed at the ocean surface, although

this is commonly believed to be the case.

One difficulty with many methods is that the restrictions on the

model are incorporated into the numerical techniques used, and the inter-

preter may not be fully aware of them. For example, the polygon methods

produce a model of a given number of sides, but do not guarantee that a

different polygon will not also be acceptable. The Cordell-Henderson method

requires a reference plane to mark the top, midpoint, or bottom of the

prisms which comprise the model. Such restrictions often necessitate an

initial model which fits the data reasonably well. For example, Cordell

and Henderson found their results to be physically plausible only for res-

tricted choices of reference plane; to obtain a reasonable spherical model,

the reference plane had to be set through the center of the sphere.

The non-uniqueness of gravity inversions is then not an insur-

mountable obstacle. It is usually possible to produce a simple model (with

a limited number of parameters) to account for any gravity anomaly; however

it will not necessarily be the only acceptable simple model. Before making

a geological interpretation, it is essential to examine the inversion method

to understand the limitations of the solution.

The availability of other geophysical or geological data can be

of great help in establishing an initial model which allows a reasonable

solution to the inverse problem. In situations where there is little prior

information, the choice of initial model may become difficult; in this case,

a method requiring few assumptions about the form of the anomalous body

would be advantageous. Some new techniques for gravity data will be deve-

loped later in hopes of finding inversions without requiring a detailed

initial model.

2.3 New Approaches to Geophysical Inverse Problems

a. The Backus-Gilbert Method

In recent years, a strong theoretical basis for geophysical

inverse problems has been established, particularly in the work of Backus

and Gilbert (1967, 1968, 1970). A major innovation is that the non-

uniqueness of inversions is exploited by seeking particular models which

satisfy the data from the Hilbert space[*] of all possible models. This can

usually be achieved by optimizing some property of the model subject to

the constraints imposed by the observations; for example, the "distance"[*]

of the model from an initial model (in a parameter space) might be minimized,

---

[*]See Appendix A.

or the average properties of adjacent models might be obtained by finding

the "smoothest" model. Some of the older inversion methods may produce

similar results, but the Backus-Gilbert approach emphasizes the true nature

of the solution; in addition, their formalism is much more flexible in that

similar algorithms can be employed to produce models of different properties.

Parker (1970) has given a good summary of their techniques.

A central concept in the Backus-Gilbert method is that models

which satisfy the data are points in a Hilbert space which includes all

possible models. In one sense, such models can not be unique for any geo-

physical data, since only a finite number of data are available, but the

earth's properties can be infinitely variable if viewed on a sufficiently

fine scale. Particular data, for example potential field observations,

may also contain other sources of non-uniqueness. A model with N parameters

(or one parameter evaluated at N spatial positions) may be considered to

lie in a N-dimensional subspace.

If the geophysical functions under consideration can be expressed

as inner products[*] defined on the Hilbert space, the Backus-Gilbert formalism

can exploit the properties of the inner product to develop a model from the

observations. A linear functional can always be written as an inner product

(Hoffman and Kunze, 1961, p. 235); non-linearity can also be handled, so

long as the functional is Frechet-differentiable[*] and can be linearized in

the region near an initial model. In geophysical inversions, this restric-

tion is usually no problem, since most earth data have been shown to be

---

[*]See Appendix A.

Frechet-differentiable; Backus and Gilbert (1967) cite several examples, including mass, moment of inertia, travel times of seismic waves, and normal mode oscillation frequencies.

The basic notation of the Backus-Gilbert method is as follows:

a) E_j^0 or γ_j are the observed data

b) $E_j(M)$ is the data functional of the model M

Frechet differentiability implies

c) $E_j(M + \Delta M) = E_j(M) + (F_j, \Delta M) + \varepsilon(\Delta M)$

d) F_j is the Frechet kernel, and $(F_j, \Delta M)$ is an inner product

e) $A = \Sigma \, a_i F_i$ is an averaging kernel for the model M

The inversion starts with computation of the Frechet kernels for the particular data functionals and model parameters. Different approaches are then available, depending on the nature of the desired solution. For example, the "distance" of an acceptable model from an initial guess can be minimized, subject to the constraints that the data functionals have certain known values. This reduces to a classical calculus of variations problem, easily solved via the Lagrangian multiplier technique (details are given in Appendix C). If the functionals are non-linear, the solution must be iterated in small linear steps from the previous model.

Another technique is to find average properties of acceptable models, using an averaging kernel which is a linear combination of the Frechet kernels. The averaging kernel is given by

$$A = \sum_i a_i F_i$$

The 1968 paper demonstrates that the average model <m> can then be expressed as a linear combination of the observations, i.e.

$$<m> = \int_V Am \, dV = \sum_i a_i \gamma_i$$

so long as the functionals are linear, or can be linearized in the neighbourhood of the average model. Establishing a criterion for the quality of the local averages leads to computational methods for determining the coefficients a_i of the averaging kernel. Backus and Gilbert (1970) minimized the "spread" of A, given by

$$S(r_o, A) = 12 \int_0^1 (r - r_o)^2 A(r)^2 \, dr$$

to determine averaging kernels for whole earth models. The basic aim of the process is to find an average with the shortest resolution length possible. The form of the averaging kernels gives an estimate of the resolving power of the inversion, ideally, $A(r)$ should be a delta function (hence the term "δ-ness criteria" in the 1968 paper).

One advantage of this approach is that the averages are unique if the model is linear; in addition, all models which are "near" to each other (in the sense that $E_j(m) - E_j(m')$ is linear in $(m-m')$, where m, m' denote different models) have the same average properties. The averaging process thus obtains unique solutions from a finite series of observations;

however it does not remove other sources of non-uniqueness. When the data

contain errors, the model averages can no longer be precisely determined.

The problem that then arises is that the standard error in <m> increases

as the resolving length decreases, i.e. there is a tradeoff between the

resolution of the averaging kernel and the standard error in the resulting

averages. In their 1970 paper, Backus and Gilbert were concerned with

computing tradeoff curves for noisy data, and with strategies which lead to

a reasonable compromise.

In some cases, the resolving power of the data may be so poor that

different models cannot effectively be distinguished. This is certainly

true for gravity data. Since the gravity-density relationship is linear

(see Chapter 3), all possible density models are "near" to one another in

the Backus-Gilbert sense. It has been noted earlier (Section 2) that quite

different models can produce the same gravity effect; the only properties

common to all models are the total (anomalous) mass, and the surface position

of the center of mass (which can easily be found from the data alone, e.g.

Grant and West, 1965, pp. 227-230).

Backus and Gilbert applied their methods to the problem of deter-

mining the density structure of the earth, and have been able to estimate

the resolution limits imposed by the finite data set available. Parker

(1970, 1972) successfully adopted their technique to model the conductivity

structure of the mantle, and to make gross estimates of the core densities

of the outer planets. Der and Landisman (1972) used the same basic approach

to produce crustal models from surface wave observations, and examined the

ability of the data to resolve density and shear velocity.

b. <u>The Generalized Inverse Approach</u>

Other authors in recent years have attempted to solve inverse

problems using the generalized inverse of a matrix (Penrose, 1955). If the

available data can be related to model parameters by a matrix equation, the

generalized inverse will give a particular model which satisfies the data,

the solution being the one of least Euclidean "length" (Smith and Franklin,

1969). Here "length" implies distance from the origin in parameter space

(see Appendix A). The usual application is to solve for corrections to

initial model parameters, which is equivalent to the Backus-Gilbert method

of minimizing "distance" between models.

The basic formulation of a generalized inverse problem is as

follows (Wiggins (1972) and Jackson (1972) give more complete details).

One seeks N model parameters P_i knowing M observations O_j of the real earth.

Changes in model parameters are related to changes in the data functional

by a matrix A' of "variational parameters".

$$[A'] \ [\Delta P'] = [\Delta C'] \tag{1}$$

where $[A_{ij}'] = [\partial C_i / \partial P_j]$

$C_i = F_i(P_j)$ is the <u>linearized</u> functional corresponding to

observation i

$\Delta C_i' = O_i - C_i$

Solving this system using the generalized inverse of A yields a set of

parameter corrections ΔP_i, such that both $|\Delta P|^2$ and $e^2 = |A\Delta P - \Delta C|^2$ are

minimized (Wiggins, 1972). If model parameters have different dimensions,

scaling is necessary to make the minimization reasonable. Error statistics

may also be incorporated in weighting. One then solves the modified system

$$A \, \Delta P = \Delta C \tag{2}$$

where $A = S^{-1/2} \, A' \, W^{1/2}$

$\Delta P = W^{-1/2} \, \Delta P'$

$\Delta C = S^{-1/2} \, \Delta C'$

S = covariance matrix of the observations

W = covariance matrix of the parameters

The inversion is performed by finding the eigenvalues and eigenvectors of A.

Three further benefits of this analysis are: near-zero eigenvalues can be

rejected to remove potential instability of the solution caused by noisy data;

the eigenvectors corresponding to columns of A are a measure of the resolution

of the parameters; and the row eigenvectors can indicate the information

distribution among the observations.

The generalized inverse method is becoming popular, since it can

easily be implemented using standard matrix techniques. Jordan and Franklin

(1971) used a variation of the basic method, and found earth density models

by considering them to be outputs of a linear filter; this formulation allows

rejection of models which are not "smooth". Jackson (1972) examined the

theoretical performance of a generalized inverse for underdetermined and

overconstrained systems. Wiggins (1972) also studied resolution in deducing

density models from surface wave and free oscillation data. Like the Backus-

Gilbert method, the generalized inverse requires linear or linearized functionals; non-linear models can be found by iterative solution of a linearized system.

Braile et al (1973) used the method to solve for the densities of multi-prism gravity models. The number, size, and position of prisms was left to the discretion of the interpreter, allowing considerable use of other data. The generalized inverse found corrections to densities of an initial model, with reasonable success in such application as a crustal model for a profile across Texas. However, their success depended on being able to construct a good initial model comprised of prisms of various sizes, and their method might not be practical in areas where little other information is available.

c. Monte Carlo Modelling

Monte Carlo techniques for geophysical modelling have become practical with the advent of large, fast digital computers. In essence, these methods construct models whose parameters are randomly distributed over specified intervals, and then test these random models to find those whose properties agree with observations of the real earth. All the acceptable models are examined to estimate the average values of model parameters, their standard deviations, and the resolving power of the data (Wiggins, 1972).

Monte Carlo methods in geophysics are usually attempts to randomly sample the space of all models which satisfy the data, in hopes of finding the bounds of acceptability. The main difficulty is that almost all of the

random models are rejected; hence the model building process must be res-

tricted to ensure finding some acceptable models, and the testing simplified

to reduce total computing time. The former is accomplished by generating

parameters randomly within the restrictions of present knowledge; for example

density values are picked in a small interval about the accepted earth models,

and usually made to increase monotonically below the upper mantle. The

testing of models against the observations usually employs linearized varia-

tional parameters rather than exact computations of non-linear functionals

(the variational parameters of Wiggins (1968) are frequently used to compute

free oscillation periods of earth models).

Monte Carlo methods are often used in problems where many different

data are to be inverted. Press (1968, 1970) considered models whose para-

meters were density, shear velocity, and compressional velocity at 88 radii

within the earth; the values were generated randomly at 23 points, and

interpolated elsewhere. Models were tested against 97 eigenperiods, various

travel time data, and the earth's mass and moment of inertia. Press found

11 acceptable models from a total of 5 million, requiring 20 hours of com-

puter time (1968). Refinements to the procedure enabled him to find 11

successes in one hour of computation (1970). Other applications have been

discussed by Keilis-Borok and Yanovskaya (1967) and Wiggins (1969) in

inversions of body-wave data, and Anderssen (1970), who sought bounds on the

conductivity of the lower mantle.

A final point of discussion is the question of whether the method

provides adequate sampling of the model space. Backus and Gilbert (1970,

p. 126) suggest that it cannot; however Press (1970) demonstrated that a small number of random models (25) can effectively span the parameter space in which they were constructed. Anderssen et al (1972) discussed several points of contention, and concluded that the various methods of inversion should be able to provide equivalent information about the earth.

CHAPTER 3

Linear Models For Gravity Data

As noted earlier (Section 2.1), the commonly-used methods for
modelling gravity data involve non-linear functionals; i.e. the parameters
of the model are not linearly related to the surface gravity. For example,
the polygon methods use the subsurface location of vertices as parameters;
and the unknowns in Tanner's models are depths to bottom of blocks. Linear
density models can be constructed, since surface gravity is a linear function
of density; the inversion techniques to be developed will apply to linear
models (densities at different locations are the only parameters). A linear
approach was inspired by the simplified methods developed for linear (or
linearized) functionals, which were discussed in Chapter 2.

Since gravity data may be measured along a line or over a surface
grid, models of the subsurface density distribution may be two-dimensional
or three-dimensional, respectively. In either case, analytic relationships
can be established to compute the gravity effect of the model; however the
two-dimensional case requires the assumption that the model has infinite
extent in the third spatial coordinate. The two-dimensional equations are
thus always an approximation, but are generally acceptable when the length
of an anomalous body is greater than about five times its width (Grant and
West, 1965). Only two-dimensional models will be considered here, for they
involve fewer parameters and are therefore more practical for testing new
techniques. The approach would be essentially the same for three-dimensional
models, but computational tests would be much more expensive. The primary

purpose is to test new modelling methods, so it will be assumed that the gravity data are exactly known; in any case, non-uniqueness precludes detailed consideration of data errors.

The gravitational potential of any mass distribution in a Cartesian system is

$$U(x,y,z) = \gamma \int_{-\infty}^{\infty} \int_{-\infty}^{\infty} \int_{-\infty}^{\infty} \frac{\rho(x_o,y_o,z_o)}{r} dx_o dy_o dz_o \qquad (1)$$

where $r^2 = [(x-x_o)^2 + (y-y_o)^2 + (z-z_o)^2]$

and γ = the gravitational constant

If a body is essentially two-dimensional, one assumes that ρ does not vary in the y_o direction, and performs one integration to obtain

$$U(x,z) = 2\gamma \int_{-\infty}^{\infty} \int_{-\infty}^{\infty} \rho(x_o,z_o) \ln(R) dx_o dz_o \qquad (2)$$

where $R^2 = (x-x_o)^2 + (z-z_o)^2$ (Grant and West, 1965, p.230)

Gravity surveys measure the vertical component of gravitational attraction at the earth's surface ($z = 0$); the vertical gravity is related to the potential by

$$g_z(x,0) = -\frac{\partial U(x,z)}{\partial z} \bigg|_{z=0}$$

hence

$$g_z(x) = 2\gamma \int_{-\infty}^{\infty} \int_{-\infty}^{\infty} \frac{z_o \rho(x_o, z_o)}{(x-x_o)^2 + z_o^2} \, dx_o dz_o$$

As noted earlier, g_z is a linear function of ρ. Linearity requires

$$F(\alpha x + y) = \alpha F(x) + F(y) \qquad \text{(Hoffman and Kunze, 1961, p. 91)}$$

From (3)

$$g_z(a\rho_1 + \rho_2) = 2\gamma \int_{-\infty}^{\infty} \int_{-\infty}^{\infty} \frac{z_o(a\rho_1 + \rho_2) \, dx_o dz_o}{(x-x_o)^2 + z_o^2}$$

or

$$g_z(a\rho_1 + \rho_2) = 2\gamma a \int_{-\infty}^{\infty} \int_{-\infty}^{\infty} \frac{z_o \rho_1 dx_o dz_o}{(x-x_o)^2 + z_o^2} + 2\gamma \int_{-\infty}^{\infty} \int_{-\infty}^{\infty} \frac{z_o \rho_2 dx_o dz_o}{(x-x_o)^2 + z_o^2}$$

$$= a g_z(\rho_1) + g_z(\rho_2) \qquad \text{Q.E.D.}$$

Knowing that (3) is linear in ρ, the Frechet kernel for g_z is immediately seen to be

$$G(x, x_o, z_o) = \frac{2\gamma z_o}{(x-x_o)^2 + z_o^2}$$

and the vertical gravity may be written as an inner product

$$g_z(x) = (G(x, x_o, z_o), \rho(x_o, z_o)) = \int_{-\infty}^{\infty} \int_{-\infty}^{\infty} G(x, x_o, z_o) \, \rho(x_o, z_o) dx_o dz_o \qquad (5)$$

$G(x, x_o, z_o)$ may also be considered to be the Green's function which generates the vertical gravity from the source term $\rho(x_o, z_o)$.

Considering g_z as a derivative of the potential, the total anomalous mass which causes g_z can be determined by an application of Gauss' theorem; for a two-dimensional body the result is

$$M = \frac{1}{4\gamma} \int_{-\infty}^{\infty} g_z(x)\,dx \qquad \text{(Grant and West, 1965, p.273)} \qquad (6)$$

All models which fit a given gravity profile must have the same excess mass, since the integral is not taken over the source region, but is related solely to the data.

Equation (3) cannot be applied directly, since an exact integration would require a knowledge of ρ at all values (x_o, z_o); the equations (3), (4), and (5) must be adapted to consider models which specify ρ at only selected values of x_o, z_o. The models used hereafter will have the form shown in Figure 1. The subsurface region underlying the gravity profile is divided into rectangular cells, centered at (x_o, z_o). The model parameters are constant densities $\rho(x_o, z_o)$ assigned to each cell; the surface gravity is then the sum of the gravity effects of each cell (again because of linearity). The integral (4) is now written as a summation

$$g_z(x_i) = \sum_j \sum_k G(x_i, x_j, z_k)\, \rho(x_j, x_k) \qquad (7)$$

provided that the Frechet kernel $G(x, x_o, z_o)$ is modified from the point mass

Gravity stations: $x_i = i*dx$
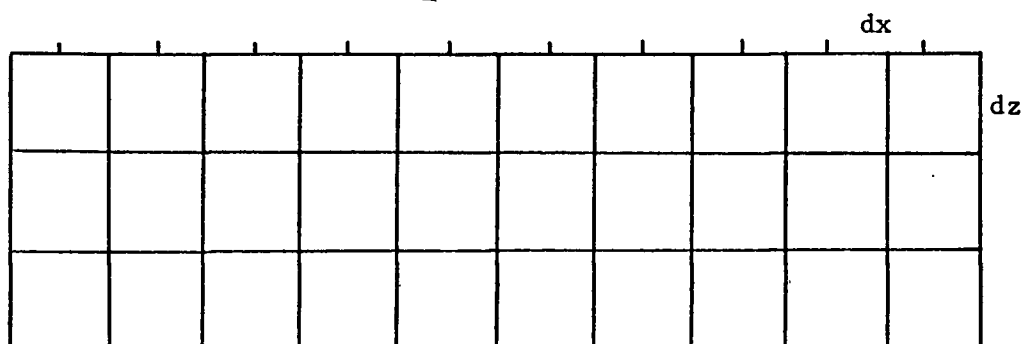
Prism centers: $x_j = j*dx$

$z_k = k*dz$

(a)   Standard Model

Gravity stations: $xx_i = i*dx$
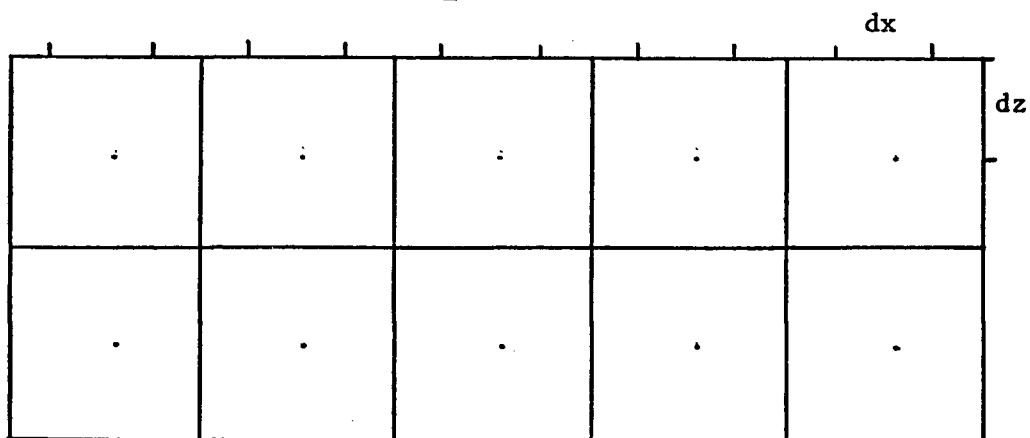
Prism centers: $x_j = (2j - 1/2)*dx$

$z_k = 2(k - 1/2)*dz$

(b)   Large-block Model

Fig. 1.   Linear models for gravity anomalies.

expression (4) to a form corresponding to a cell of dimensions dx, dz.

Mottl and Mottlova (1972) used such a regular grid in their simple two-dimensional models (using 20 to 30 cells to model a 5 point gravity profile), but restricted density to values of 0 or 1 only, and thus required an iterative method of inversion (numerical optimization of a "shape preference" function). The models of Braile et al (1973) also used prism densities as parameters to exploit linearity, but reduced the total number of parameters by using blocks of different sizes, usually much greater than the surface station spacing. The models suggested here differ in that all blocks will be of the same dimensions, generally equal to the station spacing; and the subsurface geometry will not be altered for each set of data to be inverted.

Modelling the earth with these discrete elements is a sampling process, and thus the spatial frequencies which can be represented have an upper limit. However, since the gravity data are also sampled, high frequencies of the real earth density distribution will be aliased, and the model should be able to represent all real frequencies present in the data. If prisms of dimension twice the surface spacing are used, the model cannot represent all possible frequencies in the data; such models may be adequate if large features are expected (which is usually true in gravity exploration). In either case, one must hope that the station spacing used in measuring the data is small enough to prevent a serious aliasing problem.

There are two ways to consider the nature of these models. First, they can be viewed as models of a single parameter (density), which is
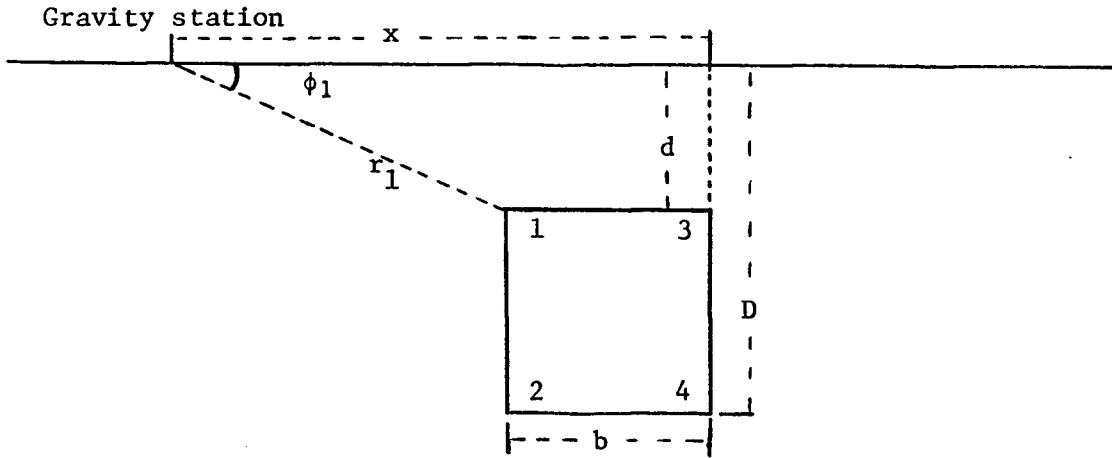
ϕ_1, ϕ_2, ϕ_3, ϕ_4 are angles to respective corners

r_1, r_2, r_3, r_4 are distances to respective corners

Fig. 2. Geometric quantities required for the gravity effect of a prism (after Parasnis, 1962, p.43).

specified at regular intervals in the subsurface plane. Alternately the density of each cell might be considered as an independent parameter, and in this case we consider properties of the N-dimensional parameter space, where N is the number of prisms in the model.

Before the models can be used, the Frechet kernels for a rectangular prism must be calculated. They are obtained from (3) by integrating only over the rectangular prism, where the density is assumed constant. Parasnis (1962, p. 44) gives the following relationship for the vertical gravity

$$g_z(x) = 2\gamma\rho \left[x\ln \frac{r_1 r_4}{r_2 r_3} + b\ln \frac{r_4}{r_1} + D(\phi_2 - \phi_4) - d(\phi_1 - \phi_3) \right] \qquad (8)$$

The various geometric quantities are shown in Figure 2. The Frechet kernel

follows immediately from (8) as

$$G(x,x_o,z_o) = \frac{g_z(x)}{\rho} \qquad (9)$$

where the geometric quantities in (8) would correspond to a prism centered at (x_o,z_o). Equations (8) and (9) give an exact expression for the Frechet kernel, but computations can be made much simpler by approximating each cell as a point mass located at its center (in the two-dimensional case, a "point" mass is of course a line mass). From (3) the gravity effect of this source is

$$g_z(x) = \frac{2\gamma z_o (\text{mass})}{(x-x_o)^2 + z_o^{\,2}} \qquad (10)$$

where the mass is equivalent to that of the prism, i.e.

$$(\text{mass}) = \rho(dx)(dz) \qquad (11)$$

which is expressed in gm/length for the two-dimensional model.

To ensure that the approximation is valid, the results of Equation (8) and (10) must be compared for different cells in the model. Since we will always employ the same geometry of cell location and have $dx = dz$, a simple correction can be made to (10) to give the same results as (8), if the agreement is not acceptable. We consider distances measured in kilometers, densities in gm/cm^3, and gravity in milligals; hence the numerical value of γ must be 6.67 (see Appendix B).

The comparison was made for prisms at various depths, and for prism

dimension 1 km or 2 km. The gravity was computed at 1 km surface intervals, with x=0 being the ground position directly above the center of the cell. The station spacing (and related prism dimension) is unimportant, as we require only the ratio of the gravity effects. The results are displayed in Table I and II. The approximation is almost always accurate within 0.5%, however for gravity stations near the surface cells, the difference is great enough to warrant a correction; as should be expected from the inverse-square nature of gravity.

The Frechet kernels for the linear model are now obtained from (10), applying the correction factor if the approximation is off by more than 0.5%. The kernel is written

$$G(i,j,k) = \frac{2\gamma \; dx \; dz \; f}{(x_i-x_j)^2 + z_k^2} \tag{12}$$

and the gravity effect at surface position x_i is

$$g_z(i) = \sum_j \sum_k G(i,j,k) \; \rho(j,k) \tag{13}$$

where $\rho(j,k)$ is the density of the prism centered at (x_j, z_k). The correction factor "f" is usually 1, the other values that were used are shown in Table III.

Using this formulation, the gravity effect of different models is obtained simply by evaluating the inner product (13) with different $\rho(j,k)$; the Frechet kernels need be computed only once and then retained for later use. In this procedure, the time saved by computing the approximate kernel

IN THE FOLLOWING TABLE "X" IS THE DISTANCE FROM
THE GROUND POSITION DIRECTLY ABOVE THE CENTER OF THE
PLATE OR CYLINDER

THE DENSITY OF THE PLATE IS   1.00
THE WIDTH OF THE PLATE IS   1.00
THE HEIGHT OF THE PLATE IS   1.00

THE DEPTH TO THE CENTER IS   0.5 KM

| | GRAVITY EFFECT (MGAL) | | | |
X (KM)	PLATE	CYLINDER	DIFFERENCE	CORRECTION FACTOR
0.0	23.1051	26.6800	-3.5749	0.86601
1.0	5.2370	5.3360	-0.0990	0.98145
2.0	1.5638	1.5694	-0.0056	0.99643
3.0	0.7204	0.7211	-0.0006	0.99912
4.0	0.4104	0.4105	-0.0001	0.99979
14.0	0.0340	0.0340	-0.0000	0.99916
15.0	0.0296	0.0296	-0.0000	0.99936

THE DEPTH TO THE CENTER IS   1.5 KM

| | GRAVITY EFFECT (MGAL) | | | |
X (KM)	PLATE	CYLINDER	DIFFERENCE	CORRECTION FACTOR
0.0	8.8645	8.8933	-0.0288	0.99676
1.0	6.1684	6.1569	0.0115	1.00187
2.0	3.2018	3.2016	0.0002	1.00005
3.0	1.7783	1.7787	-0.0004	0.99978

THE DEPTH TO THE CENTER IS   2.5 KM

| | GRAVITY EFFECT (MGAL) | | | |
X (KM)	PLATE	CYLINDER	DIFFERENCE	CORRECTION FACTOR
0.0	5.3337	5.3360	-0.0023	0.99957
1.0	4.6005	4.6000	0.0005	1.00011
2.0	3.2543	3.2537	0.0006	1.00020

THE DEPTH TO THE CENTER IS   9.5 KM

| | GRAVITY EFFECT (MGAL) | | | |
X (KM)	PLATE	CYLINDER	DIFFERENCE	CORRECTION FACTOR
0.0	1.4043	1.4042	0.0001	1.00005
1.0	1.3888	1.3888	0.0000	1.00001
2.0	1.3445	1.3446	-0.0001	0.99992
14.0	0.4428	0.4427	0.0000	1.00007
15.0	0.4018	0.4020	-0.0002	0.99959

TABLE I. Gravity effects of prisms (in the standard model) and
equivalent cylinders.

THE DENSITY OF THE PLATE IS   1.00
THE WIDTH OF THE PLATE IS   2.00
THE HEIGHT OF THE PLATE IS   2.00

THE DEPTH TO THE CENTER IS   1.0 KM

X (KM)	GRAVITY EFFECT (MGAL) PLATE	CYLINDER	DIFFERENCE	CORRECTION FACTOR
0.5	43.3750	42.6880	0.6871	1.01609
1.5	16.1710	16.4184	-0.2475	0.98493
2.5	7.2643	7.3600	-0.0957	0.98700
3.5	4.0053	4.0272	-0.0218	0.99458
4.5	2.5050	2.5111	-0.0061	0.99757
5.5	1.7055	1.7075	-0.0020	0.99880
6.5	1.2329	1.2338	-0.0008	0.99934
7.5	0.9317	0.9321	-0.0003	0.99964
8.5	0.7283	0.7285	-0.0002	0.99973
9.5	0.5847	0.5848	-0.0001	0.99982
10.5	0.4796	0.4796	-0.0001	0.99986

THE DEPTH TO THE CENTER IS   3.0 KM

X (KM)	GRAVITY EFFECT (MGAL) PLATE	CYLINDER	DIFFERENCE	CORRECTION FACTOR
0.5	17.2690	17.3059	-0.0369	0.99787
1.5	14.2519	14.2293	0.0226	1.00159
2.5	10.5119	10.4970	0.0149	1.00142
3.5	7.5358	7.5332	0.0026	1.00035
4.5	5.4722	5.4728	-0.0006	0.99988
5.5	4.0776	4.0785	-0.0009	0.99978
6.5	3.1229	3.1235	-0.0007	0.99979
7.5	2.4529	2.4533	-0.0004	0.99983

THE DEPTH TO THE CENTER IS   5.0 KM

X (KM)	GRAVITY EFFECT (MGAL) PLATE	CYLINDER	DIFFERENCE	CORRECTION FACTOR
0.5	10.5624	10.5663	-0.0039	0.99963
1.5	9.7904	9.7908	-0.0004	0.99996
2.5	8.5394	8.5376	0.0018	1.00021
3.5	7.1640	7.1624	0.0016	1.00023
4.5	5.8970	5.8961	0.0009	1.00014
5.5	4.8292	4.8290	0.0003	1.00005
6.5	3.9673	3.9673	0.0000	1.00000
7.5	3.2836	3.2837	-0.0001	0.99997

TABLE II.   Gravity effects of prisms (in the large-block models)
and equivalent cylinders.

Standard model: z_n, x_m = subsurface position

x_j = surface position

$\underline{n}$	$\underline{|j-m|}$	$\underline{f}$
1	0	0.86601
1	1	0.98145
2	0	0.99676

Large-block model: xx_j = surface position

define $XA = |x_m - xx_j|/dx$

$\underline{n}$	$\underline{XA}$	$\underline{f}$
1	0.5	1.01609
1	1.5	0.98493
1	2.5	0.98700
1	3.5	0.99458
2	0.5	0.99787

Note: These values are valid only for $dx = dz$ in Figure 1.

TABLE III.   Correction factors used in computing Frechet kernels.

may not be important, particularly if a large computer is available. On

the IBM 360/67, about 5 seconds would be used in computing the exact kernels

for a 300 cell model and a 30 station profile; the approximate kernels are

obtained in about 1/25 of this time (0.2 sec.).

The calculations in Tables I and II also demonstrate that isolated

anomalies need not be modelled to a great depth (relative to the profile

length). If a residual anomaly is to be nearly zero at the ends of the

profile, prisms at a depth greater than about one-third the profile length

cannot make a significant contribution to the gravity. For example, a unit

cell at depth 9.5 km. has a gravity effect of 1.4 mgal at $x = 0$ km., and

0.4 mgal at $x = 15$ km., a ratio of only 3.5; we conclude that a cell at that

depth cannot make a large contribution at the center of the profile, if the

total gravity at the end of the profile is small. For this reason, the

models studied later will have a maximum cell depth of $z = 9.5$ (to center)

for a 30-unit profile length. From similar considerations, in many cases

cells near the ends of the profile need not be considered.

We can now summarize the advantages of the suggested linear

density models. Linearity is the main benefit; it allows easy computation

of the gravity of any model from the Frechet kernels. The point mass

(actually line mass) approximation simplifies the computation of the kernels.

If an initial model is used, a model which fits the data can be obtained in

one step. Unfortunately, there are two major disadvantages. Since the

model consists of blocks, only rough approximations to complex shapes are

possible; however most gravity methods share this difficulty, since the

non-uniqueness problem prevents precise gravity interpretation. The variable

density between blocks of the model may obscure geological interpretation,

as the inversion will not necessarily indicate an anomalous structure of only

one or two densities. In most uses of gravity exploration, a single-density

model is desired, as the exploration objective is usually a body of a speci-

fic mineral ore, whose density should be essentially constant. The inversion

procedures tested here will therefore attempt to find models in which the

density contrast of individual cells is either zero or a constant value, in hopes of defining a simple anomalous body.

CHAPTER 4

Backus-Gilbert Approaches To Gravity Modelling

The techniques developed by Backus and Gilbert have mainly been used to construct models of the whole earth, but there is no inherent limitation against using them for more restricted examples. In particular, linear density models of the type proposed in Chapter 3 are easily obtained from Backus-Gilbert inversions.

It was previously observed (Section 2.3.a) that the averaging procedures used by Backus and Gilbert are not of much benefit to the suggested gravity models, since all linear models have the same average properties, and the only unique properties obtainable from gravity data are the total mass and center of mass coordinates. For this reason, attention will be confined to the technique of finding particular models by optimizing some property of the model under the constraints imposed by the observations (in the present case, values of the vertical gravity component at specific points along a surface profile). The inherent lack of resolution of gravity data also prevents any extensive analysis of the effects of data errors on the models obtained. The approach used here is merely to seek approximate density models which satisfy a gravity anomaly within a specified error.

The generalized inverse gives results equivalent to the Backus-Gilbert "distance" minimization. For the proposed gravity models, the Backus-Gilbert formulation is more compact, since taking inner products reduces the dimension of matrices which need to be inverted. The generalized

inverse uses a matrix of dimension N, where N is the number of parameters; while the inner product matrix of a Backus-Gilbert inverse has dimension K, where K is the number of data. In addition, the error and resolution analyses of the generalized inverse cannot be used to full advantage. The generalized inverse was thus not pursued further.

4.1 Models "Closest" to an Initial Estimate

The first method (following Backus and Gilbert, 1967) is to find the model closest to an initial guess. The solution is obtained by minimizing the distance of an acceptable model from a given intial model; the constraints imposed by the observed gravity are incorporated via Lagrange multipliers. We then seek a stationary point of

$$F = \frac{1}{2} ||M-M_G||^2 - \sum_1^J \alpha_j \, [g_j(M_G) - \lambda_j + (G_j, M-M_G)]$$

where M, M_G denote the final and initial models

G_j is the Frechet kernel for gravity at station j

λ_j = gravity observed at station j

$g_j(M_G)$ = gravity of initial model

$(G_j, M-M_G)$ denotes an inner product

J = number of gravity data used

α_j are Lagrange multipliers

and the factor $\frac{1}{2}$ will cancel out later

There are two basic steps in the inversion; first, solve for the Lagrange multipliers α_k in

$$\sum_k \alpha_k (G_j, G_k) = \lambda_j - g_j(M_G) \tag{1}$$

For the linear models of Figure 1a, the inner product (G_j, G_k) is

$$(G_j, G_k) = \sum_n \sum_m G_{jnm} G_{knm}$$

where [n,m] defines the subsurface position of each prism. The model M which satisfies the data is now given by

$$M = M_G + \sum_1^J \alpha_k G_k \tag{2}$$

To find the densities for each block in the model, (2) is computed for each subsurface position x_m, z_n. A complete derivation of these equations is given in Appendix C.

The system of equations (1) and (2) is easily programmed for digital computer application. The spacing of gravity stations is specified to establish the size and position of cells in the model, and to compute the Frechet kernels. Given regularly-spaced gravity observations, and a set of initial densities for each prism, an exact inverse is obtained immediately. Since the models are linear, any initial model will still yield a solution which fits the data.

To test the program, a gravity profile was computed for the artificial body shown in Figure 3. It is a fairly complex object, and should provide a reasonable example for inversions which cannot indicate the precise
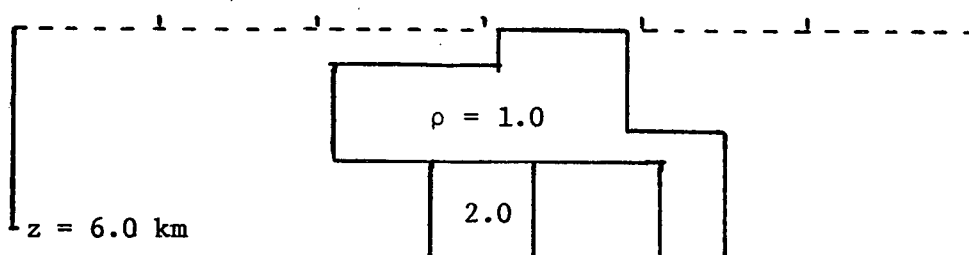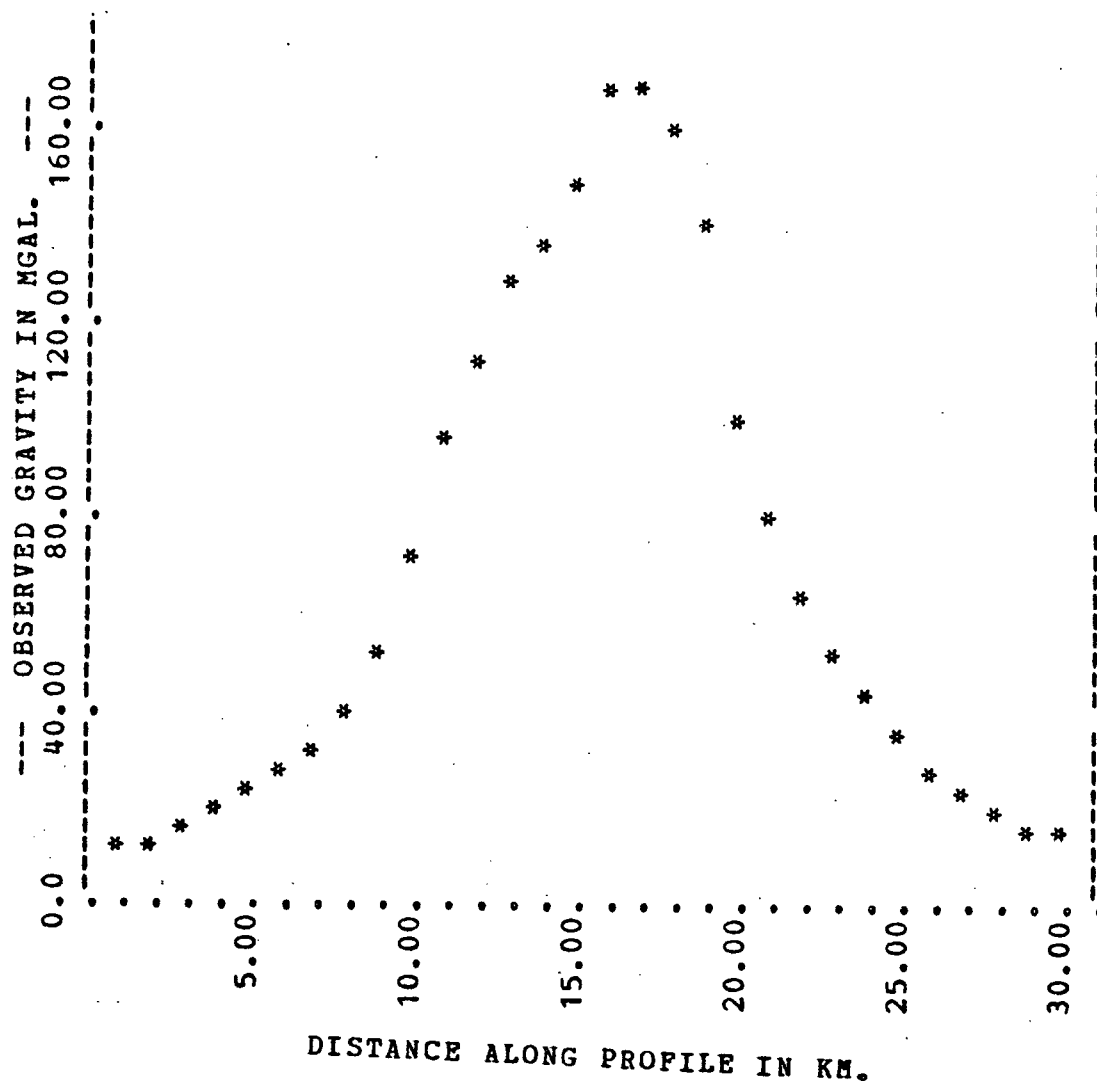
(a) Shape of the anomalous body.

Fig. 3. An artificial gravity profile.

INITIAL MODEL

X (KM) / Z=	0.50	1.50	2.50	3.50	4.50	5.50	6.50
8.00 :	0.0	0.0	0.0	0.0	0.0	0.0	0.0
9.00 :	0.0	0.0	0.0	0.0	0.0	0.0	0.0
10.00 :	0.0	0.0	0.0	0.0	0.0	0.0	0.0
11.00 :	0.0	1.000	1.000	1.000	0.0	0.0	0.0
12.00 :	0.0	1.000	1.000	1.000	0.0	0.0	0.0
13.00 :	0.0	1.000	1.000	1.000	0.0	0.0	0.0
14.00 :	0.0	1.000	1.000	1.000	2.000	2.000	2.000
15.00 :	0.0	1.000	1.000	1.000	2.000	2.000	2.000
16.00 :	1.000	1.000	1.000	1.000	2.000	2.000	2.000
17.00 :	1.000	1.000	1.000	1.000	0.0	0.0	0.0
18.00 :	1.000	1.000	1.000	1.000	0.0	0.0	0.0
19.00 :	1.000	1.000	1.000	1.000	0.0	0.0	0.0
20.00 :	0.0	0.0	0.0	1.000	0.0	0.0	0.0
21.00 :	0.0	0.0	0.0	1.000	1.000	1.000	1.000
22.00 :	0.0	0.0	0.0	1.000	1.000	1.000	1.000
23.00 :	0.0	0.0	0.0	0.0	0.0	0.0	0.0

(b) Computer representation of the body.

detail of the earth. Figure 4 shows the model obtained by using a "zero"

initial model. The inverse solution cannot be represented as an anomalous

body, since the computed densities are different for each subsurface prism.

A related problem is that no restrictions on density are built into the

program, and both negative and positive densities are obtained, particularly

on the edges of the model region. In most exploration situations, it would

be reasonable to assume that a body of constant density contrast is causing

the gravity anomaly. To reduce the ambiguity of the solutions, different

strategies were employed to seek constant density models.

A surface gravity profile should extend beyond the limits of an

anomalous body, if the gravity anomaly is to be completely defined. It is

therefore reasonable to consider models which span a region only under the

center of the profile. This is simply achieved by specifying limits on x_m

and z_n, which reduces the number of parameters and thus should help remove

negative densities (in the case of positive anomalies), since the constraint

of known mass must also be satisfied. Figure 5 shows the inversion obtained

by using a model of 105 prisms, rather than 300 as in Figure 4. Variable

density is still present, but sharp changes in density are evident, parti-

cularly in the near-surface region of the model.

To transform these models into a rough picture of a single-density

body, a program was written to replace the exact densities by discrete

values at a specified increment, simultaneously rejecting any negative

values. The resulting approximate models do not satisfy the observed gra-

vity values precisely; however they can indicate the extent and general shape

COMPUTED DENSITIES

X (KM) / Z=	0.50	1.50	2.50	3.50	4.50	5.50	6.50	7.50	8.50	9.50
1.00 :	-0.127	-0.063	-0.036	-0.016	0.001	0.016	0.028	0.039	0.047	0.054
2.00 :	-0.096	-0.072	-0.043	-0.019	0.002	0.019	0.033	0.045	0.055	0.062
3.00 :	-0.104	-0.076	-0.046	-0.018	0.006	0.025	0.041	0.054	0.064	0.071
4.00 :	-0.118	-0.081	-0.045	-0.013	0.014	0.036	0.053	0.066	0.075	0.082
5.00 :	-0.135	-0.086	-0.041	-0.003	0.027	0.051	0.068	0.081	0.090	0.096
6.00 :	-0.153	-0.086	-0.030	0.015	0.048	0.072	0.088	0.100	0.107	0.111
7.00 :	-0.167	-0.075	-0.005	0.044	0.078	0.100	0.114	0.123	0.127	0.129
8.00 :	-0.164	-0.040	0.039	0.089	0.118	0.136	0.145	0.149	0.150	0.148
9.00 :	-0.111	0.040	0.114	0.152	0.171	0.180	0.182	0.180	0.175	0.169
10.00 :	0.089	0.187	0.221	0.233	0.234	0.230	0.222	0.212	0.202	0.191
11.00 :	0.455	0.378	0.346	0.324	0.303	0.283	0.264	0.245	0.228	0.212
12.00 :	0.684	0.542	0.466	0.414	0.372	0.336	0.305	0.277	0.253	0.232
13.00 :	0.776	0.651	0.565	0.495	0.435	0.384	0.342	0.306	0.275	0.250
14.00 :	0.791	0.727	0.650	0.565	0.489	0.425	0.372	0.329	0.293	0.263
15.00 :	0.720	0.846	0.739	0.626	0.531	0.454	0.393	0.344	0.304	0.272
16.00 :	1.582	1.050	0.820	0.666	0.553	0.467	0.402	0.350	0.309	0.275
17.00 :	1.452	1.099	0.839	0.667	0.548	0.462	0.396	0.346	0.305	0.272
18.00 :	1.366	1.013	0.772	0.618	0.512	0.436	0.377	0.331	0.294	0.264
19.00 :	1.255	0.784	0.623	0.523	0.449	0.392	0.346	0.308	0.277	0.251
20.00 :	0.061	0.405	0.430	0.405	0.370	0.337	0.306	0.278	0.254	0.233
21.00 :	-0.010	0.181	0.268	0.292	0.290	0.278	0.262	0.245	0.229	0.213
22.00 :	-0.022	0.085	0.162	0.203	0.220	0.223	0.219	0.212	0.202	0.192
23.00 :	-0.048	0.029	0.093	0.136	0.162	0.175	0.180	0.180	0.176	0.171
24.00 :	-0.078	-0.010	0.046	0.088	0.117	0.135	0.146	0.150	0.152	0.150
25.00 :	-0.099	-0.037	0.013	0.053	0.082	0.103	0.117	0.125	0.130	0.131
26.00 :	-0.106	-0.053	-0.008	0.028	0.056	0.078	0.093	0.104	0.110	0.114
27.00 :	-0.105	-0.061	-0.022	0.011	0.038	0.059	0.075	0.086	0.094	0.099
28.00 :	-0.100	-0.064	-0.029	0.000	0.025	0.045	0.060	0.072	0.081	0.087
29.00 :	-0.097	-0.065	-0.032	-0.005	0.017	0.035	0.049	0.061	0.069	0.076
30.00 :	-0.128	-0.058	-0.028	-0.005	0.013	0.029	0.041	0.052	0.060	0.067

Fig. 4. An inversion of the artificial profile using a zero initial model.

COMPUTED DENSITIES

X (KM) / Z=	0.50	1.50	2.50	3.50	4.50	5.50	6.50
8.00 :	0.011	-0.043	0.240	-0.105	-0.319	-0.210	0.105
9.00 :	0.044	0.010	0.032	-0.014	-0.029	0.083	0.311
10.00 :	0.131	-0.078	-0.033	0.029	0.115	0.255	0.456
11.00 :	0.257	0.723	0.910	1.053	0.196	0.362	0.559
12.00 :	0.369	0.654	0.885	1.074	0.252	0.437	0.636
13.00 :	0.435	0.570	0.899	1.105	0.299	0.495	0.698
14.00 :	0.441	0.706	0.941	1.146	0.344	0.544	0.751
15.00 :	0.364	0.807	1.010	1.194	0.385	0.586	0.796
16.00 :	1.217	1.003	1.084	1.233	0.415	0.618	0.835
17.00 :	1.082	1.049	1.104	1.241	0.426	0.637	0.864
18.00 :	0.998	0.967	1.042	1.204	0.412	0.641	0.883
19.00 :	0.910	0.746	0.895	1.125	0.380	0.634	0.891
20.00 :	-0.212	0.366	0.674	1.025	0.354	0.625	0.884
21.00 :	-0.155	0.073	0.350	0.970	0.398	0.626	0.846
22.00 :	-0.034	-0.110	-0.511	1.275	0.654	0.610	0.717

Initial model: density 1.0 in 48 prisms ($11 \leqslant x \leqslant 22$, $0.5 \leqslant z \leqslant 3.5$)

Fig. 5. A more restricted model for Figure 3.

APPROXIMATE DENSITIES

X / Z=	0.50	1.50	2.50	3.50	4.50	5.50	6.50
8.00 :	0.0	0.0	0.0	0.0	0.0	0.0	0.0
9.00 :	0.0	0.0	0.0	0.0	0.0	0.0	0.0
10.00 :	0.0	0.0	0.0	0.0	0.0	0.0	0.0
11.00 :	0.0	1.00	1.00	1.00	0.0	0.0	1.00
12.00 :	0.0	1.00	1.00	1.00	0.0	0.0	1.00
13.00 :	0.0	1.00	1.00	1.00	0.0	0.0	1.00
14.00 :	0.0	1.00	1.00	1.00	0.0	1.00	1.00
15.00 :	0.0	1.00	1.00	1.00	0.0	1.00	1.00
16.00 :	1.00	1.00	1.00	1.00	0.0	1.00	1.00
17.00 :	1.00	1.00	1.00	1.00	0.0	1.00	1.00
18.00 :	1.00	1.00	1.00	1.00	0.0	1.00	1.00
19.00 :	1.00	1.00	1.00	1.00	0.0	1.00	1.00
20.00 :	0.0	0.0	1.00	1.00	0.0	1.00	1.00
21.00 :	0.0	0.0	0.0	1.00	0.0	1.00	1.00
22.00 :	0.0	0.0	0.0	1.00	1.00	1.00	1.00

EXACT GRAVITY - APPROX GRAVITY - ERROR

1	12.1100	11.7917	0.3183
2	13.8700	13.4755	0.3945
3	16.0400	15.5472	0.4928
4	18.7600	18.1360	0.6239
5	22.2500	21.4309	0.8191
6	26.8200	25.7176	1.1024
7	32.9700	31.4474	1.5226
8	41.5300	39.3640	2.1660
9	53.8500	50.7185	3.1315
10	71.8000	67.2621	4.5379
11	94.1600	87.7264	6.4336
12	113.2600	104.4841	8.7759
13	127.2900	116.2606	11.0294
14	137.4700	125.0552	12.4148
15	146.6200	134.5364	12.0836
16	168.8500	159.1159	9.7341
17	168.5000	162.6880	5.8120
18	159.3200	158.0511	1.2688
19	140.4500	143.3264	-2.8764
20	99.3600	104.7375	-5.3775
21	78.6500	84.1919	-5.5419
22	64.7900	69.3524	-4.5624
23	53.4800	57.0884	-3.6084
24	43.9100	46.8110	-2.9010
25	36.0500	38.4215	-2.3715
26	29.7800	31.7336	-1.9536
27	24.8300	26.4540	-1.6240
28	20.9300	22.2833	-1.3533
29	17.8300	18.9673	-1.1373
30	15.3400	16.3065	-0.9665

Fig. 6. Approximate model derived from Figure 5.

of an anomalous body. In some cases, the approximate gravity profile fits the real values within 10%, a degree of accuracy which may be satisfactory in modelling exploration data (C. Ager, personal communication, 1973). Approximate models (for the inversion shown in Figure 5) and their gravity effects are given by Figure 6. These approximations are not always geologically realistic; in the example shown, the deeper section of the model is not connected to the near-surface features.

The distance-minimization algorithm of Equations (1) and (2) can also be used for the simpler models consisting of larger prisms (dimension two station spacings), illustrated in Figure 1. These models are of course a poorer means of representing a complex geological formation, but could be useful in estimating gross features. The computer program is very similar, with only the adaptations necessary for different geometry. Equations (1) and (2) have the identical form here; the differences in size and position of blocks are incorporated in the Frechet kernels. As before, approximate solutions are constructed as an aid in interpretation.

Attempts to invert the previously-used artificial data with the simpler models were not successful. The usual results were very unrealistic models, with large positive and negative densities. One such example is shown in Figure 7.

To test the validity of the method, artificial data were generated from simple bodies which can be exactly described by a number of these large prisms; two examples are shown in Figure 8. Inversions of these data were

COMPUTED DENSITIES

X (KM) / Z=	1.00	3.00	5.00	7.00
1.50 :	-0.238	4.101	-2.729	-2.922
3.50 :	-0.024	-0.942	-0.884	-1.495
5.50 :	-0.226	3.184	0.120	-0.647
7.50 :	-0.026	-1.962	-0.148	-0.227
9.50 :	-0.228	1.947	0.402	0.135
11.50 :	0.028	-0.767	0.511	0.450
13.50 :	-0.168	3.642	1.049	0.772
15.50 :	-0.267	-4.920	0.973	1.110
17.50 :	-1.562	14.342	3.280	1.438
19.50 :	-0.279	-4.824	0.602	0.985
21.50 :	-0.010	-0.092	0.100	0.608
23.50 :	-0.026	-0.123	0.080	0.482
25.50 :	-0.017	-0.074	-0.250	0.400
27.50 :	-0.019	0.432	-1.832	0.510

OBSERVED GRAVITY - MODEL GRAVITY - ERROR

1	12.1100	12.1081	-0.0019
2	13.8700	13.8557	-0.0143
3	16.0400	16.0697	0.0297
4	18.7600	18.7783	0.0183
5	22.2500	22.1984	-0.0516
6	26.8200	26.8416	0.0216
7	32.9700	33.0330	0.0630
8	41.5300	41.5146	-0.0154
9	53.8500	53.8385	-0.0115
10	71.8000	71.8266	0.0266
11	94.1600	94.1672	0.0072
12	113.2600	113.2385	-0.0215
13	127.2900	127.2491	-0.0409
14	137.4700	137.4915	0.0215
15	146.6200	146.6283	0.0083
16	168.8500	168.8568	0.0068
17	168.5000	168.4854	-0.0146
18	159.3200	159.3201	0.0001
19	140.4500	140.5591	0.1091
20	99.3600	99.4003	0.0403
21	78.6500	78.6886	0.0386
22	64.7900	64.8147	0.0247
23	53.4800	53.5144	0.0344
24	43.9100	43.9765	0.0665
25	36.0500	36.1273	0.0773
26	29.7800	29.8009	0.0209
27	24.8300	24.9238	0.0938
28	20.9300	20.9478	0.0178
29	17.8300	17.9088	0.0788
30	15.3400	15.4146	0.0746

Fig. 7. An unsuccessful inversion using a large-block model.
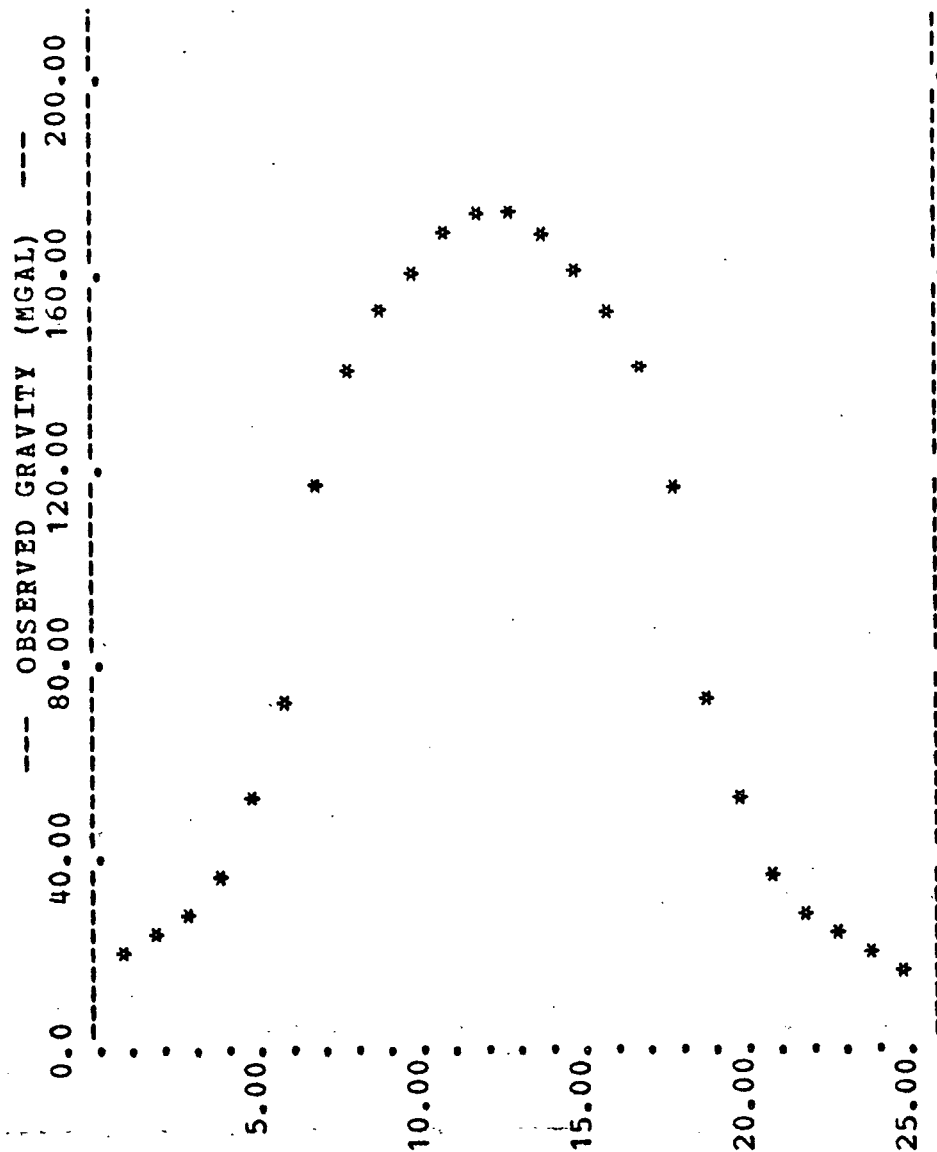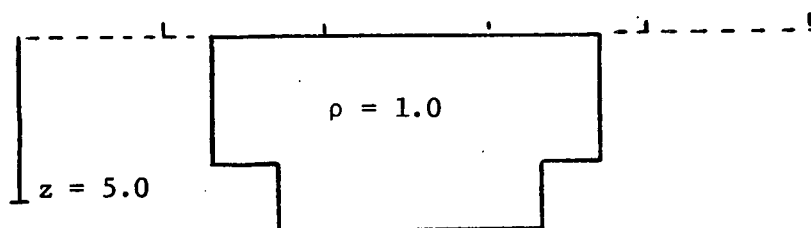
Fig. 8. Simple bodies composed of large prisms.

OBSERVED GRAVITY (MGAL)

DISTANCE ALONG PROFILE IN KM.

z = 5.0

ρ = 1.0

(b)
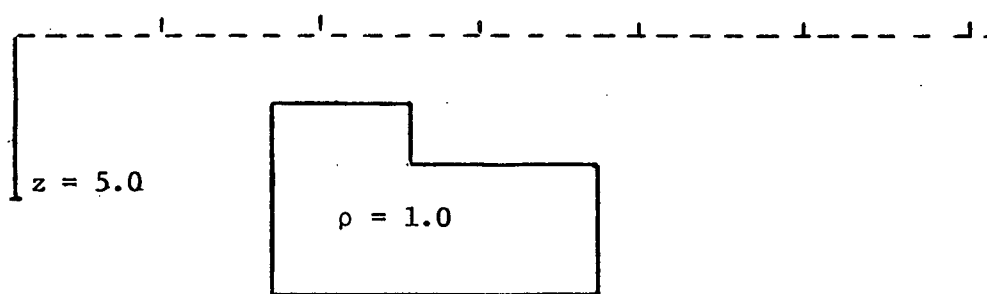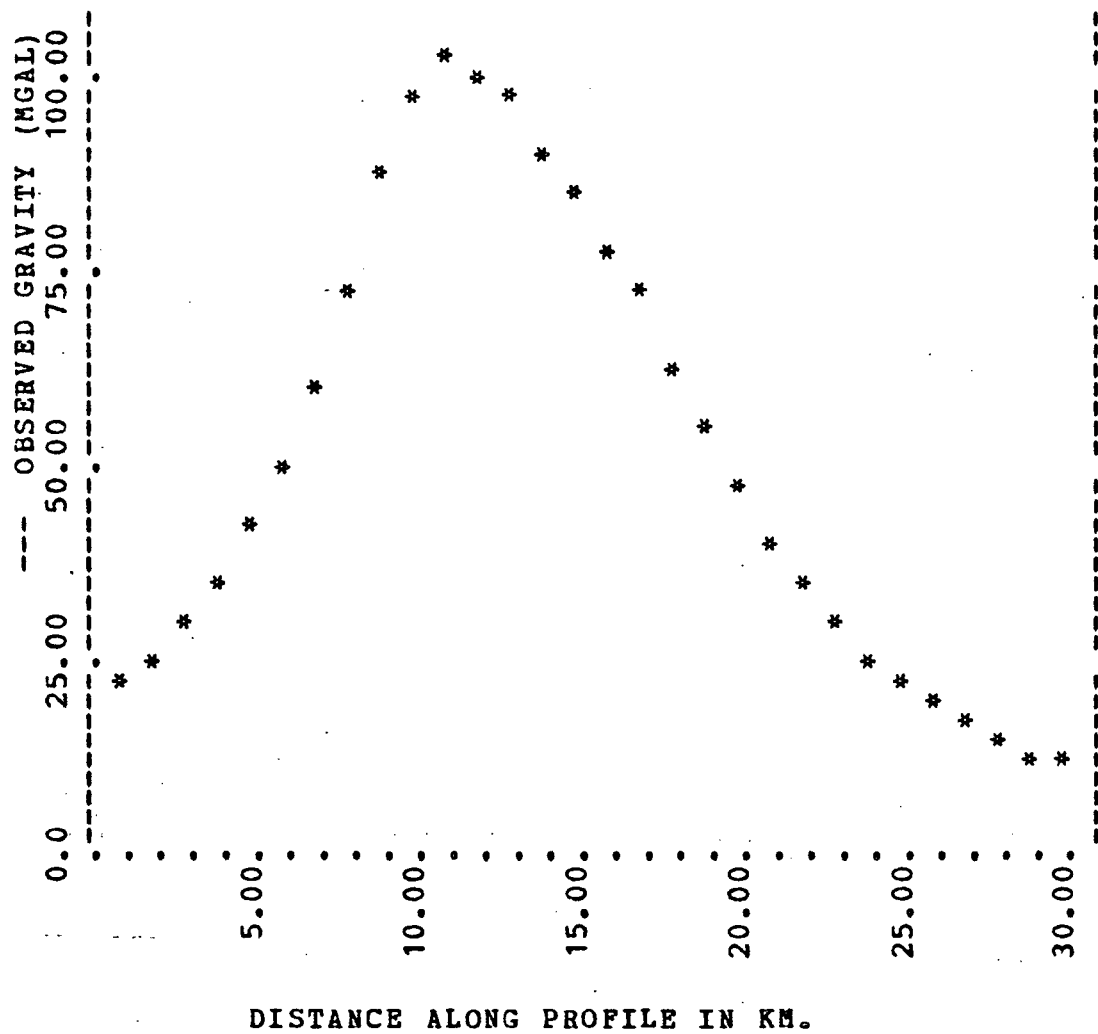
COMPUTED DENSITIES

X (KM) / Z=	1.00	3.00	5.00	7.00
3.50 :	-0.002	0.049	-0.222	-0.239
5.50 :	0.000	-0.107	0.057	0.006
7.50 :	0.999	0.851	0.410	0.223
9.50 :	0.999	0.921	0.603	0.375
11.50 :	0.998	0.992	0.679	0.450
13.50 :	1.001	0.937	0.676	0.457
15.50 :	0.998	0.937	0.609	0.401
17.50 :	1.002	0.757	0.421	0.280
19.50 :	-0.001	-0.138	0.116	0.120
21.50 :	0.000	-0.061	-0.041	-0.025
23.50 :	-0.002	0.058	-0.203	-0.163

Initial model: all zero.

APPROXIMATE DENSITIES

X (KM) / Z=	1.00	3.00	5.00	7.00
3.50 :	0.0	0.0	0.0	0.0
5.50 :	0.0	0.0	0.0	0.0
7.50 :	1.00	1.00	0.0	0.0
9.50 :	1.00	1.00	1.00	0.0
11.50 :	1.00	1.00	1.00	0.0
13.50 :	1.00	1.00	1.00	0.0
15.50 :	1.00	1.00	1.00	0.0
17.50 :	1.00	1.00	0.0	0.0
19.50 :	0.0	0.0	0.0	0.0
21.50 :	0.0	0.0	0.0	0.0
23.50 :	0.0	0.0	0.0	0.0

Fig. 9.   Inversion of data from Figure 8(a).

COMPUTED DENSITIES

X (KM) / Z=	1.00	3.00	5.00	7.00
1.50 :	-0.005	0.036	-0.026	0.019
3.50 :	-0.002	-0.051	0.038	0.089
5.50 :	-0.004	-0.005	0.127	0.183
7.50 :	-0.001	0.011	0.324	0.319
9.50 :	-0.004	1.311	0.700	0.471
11.50 :	-0.001	1.407	0.796	0.533
13.50 :	-0.003	0.565	0.610	0.489
15.50 :	-0.002	0.562	0.486	0.412
17.50 :	-0.003	0.489	0.373	0.326
19.50 :	0.001	0.137	0.221	0.235
21.50 :	-0.001	0.028	0.116	0.160
23.50 :	0.000	-0.036	0.058	0.111
25.50 :	-0.000	-0.020	0.037	0.086
27.50 :	0.001	-0.037	0.032	0.082

First result from zero initial model.

INITIAL MODEL

X (KM) / Z=	1.00	3.00	5.00	7.00
3.50 :	0.0	0.0	0.0	0.0
5.50 :	0.0	0.0	0.0	0.0
7.50 :	0.0	0.0	0.0	0.0
9.50 :	0.0	1.000	1.000	1.000
11.50 :	0.0	1.000	1.000	1.000
13.50 :	0.0	0.0	0.0	1.000
15.50 :	0.0	0.0	0.0	1.000
17.50 :	0.0	0.0	0.0	1.000
19.50 :	0.0	0.0	0.0	0.0
21.50 :	0.0	0.0	0.0	0.0
23.50 :	0.0	0.0	0.0	0.0

APPROXIMATE DENSITIES

X (KM) / Z=	1.00	3.00	5.00	7.00
3.50 :	0.0	0.0	0.0	0.0
5.50 :	0.0	0.0	0.0	0.0
7.50 :	0.0	0.0	0.0	0.10
9.50 :	0.0	1.00	1.10	1.10
11.50 :	0.0	1.00	1.10	1.10
13.50 :	0.0	0.30	0.20	1.20
15.50 :	0.0	0.40	0.20	1.20
17.50 :	0.0	0.30	0.20	1.20
19.50 :	0.0	0.10	0.10	0.20
21.50 :	0.0	0.0	0.0	0.10
23.50 :	0.0	0.0	0.0	0.0

Final result.

Fig. 10. Inversion of data from Figure 8(b).

very successful. Figure 9 shows the inversion of the data from Figure 8a; the approximate solution, starting from a zero initial model, corresponds exactly to the body which produced the data. Figure 10 illustrates the inversion of data from Figure 8b. Starting from a zero initial model, the process was repeated three times, using prior results to improve the initial model in each case. A shape corresponding to Figure 8b can be inferred from the final result. The more immediate success of the first example is probably a result of density being concentrated near the surface. The surface blocks naturally have the greatest unit contribution to the gravity; and thus their densities are most critical in fitting the data. In Figures 9 and 10, the computed densities of surface prisms are usually very close to the densities of the "real" body, regardless of the initial model.

Two basic conclusions follow from these results. Firstly, the use of large-block models yields a more nearly unique inverse, since approximate models which precisely fit the data can sometimes be obtained in one step. However, in inverting data from more complex structures, the simple model inverse is often unrealistic; this is likely a manifestation of an aliasing problem. It appears that when the data contain frequencies which cannot be represented by the model, a physically unrealistic solution will result. The problem arises from the lower cutoff wavenumber of the large-block models; i.e. the model cannot sample the subsurface density as finely as the observations sample the gravity field.

4.2 A Method of "Weighted-Distance" Minimization

In seeking a model to represent a constant density body, one hopes

to find compact configurations of the subsurface density in the linear model. Using models with restricted spatial range was one attempt in this direction; another is to establish some criterion for compactness, and then devise a scheme to select a particular model satisfying that criterion. The Backus-Gilbert method lends itself to this approach, if a simple property of the model can be optimized.

A simple view of compactness is that anomalous density should be confined as much as possible to a restricted subsurface region. A simple method is then to minimize

$$I = \int_V \rho^2 R^2 \, dV \qquad (3)$$

where R is a variable weighting factor, which is smallest in the most favoured subsurface regions. Following an anlytic procedure similar to that of Section 4.1, the following system is obtained. The Lagrange multipliers are the solution of

$$\sum_k^J \alpha_k \left(\frac{G_j}{R} , \frac{G_k}{R} \right) = \lambda_j \qquad (4)$$

and the acceptable model is given by

$$\rho = \sum_1^{J} \alpha_k \frac{G_k}{R^2} \qquad (5)$$

Equation (5) is evaluated at each x_m, z_n to give all the prism densities. A more complete derivation is shown in Appendix C.

In the form (4) and (5), it is difficult to use the system repetively to improve the first solution; so it is modified to allow use of initial models as well. Any $R(x_m, z_n)$ can be used in (4) and (5), so long as it is not a function of $\rho(x_m, z_n)$. To allow interactive use of the method, we consider R as an arbitrary weighting factor applied to each cell in the model, and minimize the weighted "distance" of an acceptable model from an initial guess. This use of R is somewhat akin to the penalty functions of some optimization methods (see Appendix D); one possible application is to maintain certain densities at their initial value. We now obtain the Lagrange multipliers by solving

$$\sum_{k=1}^{J} \alpha_k \left(\frac{G_j}{R}, \frac{G_k}{R} \right) = \lambda_j - g_j(M_G) \tag{6}$$

With the resultant model being

$$\rho = \rho_G + \sum_{1}^{J} \alpha_k \frac{G_k}{R^2} \tag{7}$$

The "weighted-distance" method is more effective than the previous examples, since one can improve an intial model while discriminating against those prisms which do not appear to contribute strongly to the anomaly. It is also a convenient way of keeping certain blocks at a known density. The computer program, listed in Appendix F as WEIGHT and SMOOTH, is of course similar to the previous ones, but requiring additional input to establish the weighting factors. Rather than specifying the numerical weight for each cell, a choice of four factors is allowed. A weight of 1.0, WT, WT2, or WT3, is assigned, depending on whether the indicator REG(N,M) is 0.0, 1.0, 2.0,

or 3.0 respectively. This method allows a simple display of variously weighted regions, and facilitates the use of different numerical factors in the same region of the model.

The program was used to invert artificial gravity profiles, two of which were generated by the simple bodies in Figure 11. Four or five repetitions of the inversion were usually sufficient to construct a reasonable single-density model. Improvement in the final stages was often a trial-and-error interpretive process; however the initial inversion from very simple models was the key to finding an acceptable solution. In all cases, application was directed towards finding a body of a single known density; in any gravity exploration, some density estimate should be available, even if it is just a guess to be tested.

Inversions of the artificial data are illustrated in Figures 12, 13, 14, and 15. The starting models were very simple; zero density for the data of Figure 11a; a large block of density 0.5 gm/cc for 11b. The first inversions were improved, partly by interpretive judgement, and partly through subsequent use of the program. In later stages, weighting factors are applied to keep certain prisms at zero density, for example, those on the boundaries of the subsurface region. Figure 12 shows the initial inversion and an intermediate stage for the data of Figure 11a, the final model after five repetitions of the program is displayed in Figure 13. The model's gravity and the "real" data usually agree within 1.0 mgal; the worst error is less than 3.0 mgal.

Figure 14 and 15 show the corresponding steps in inverting the
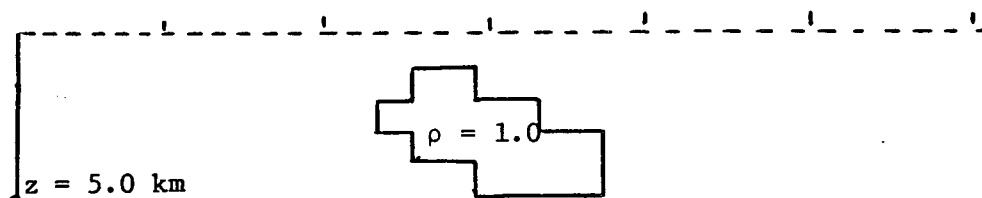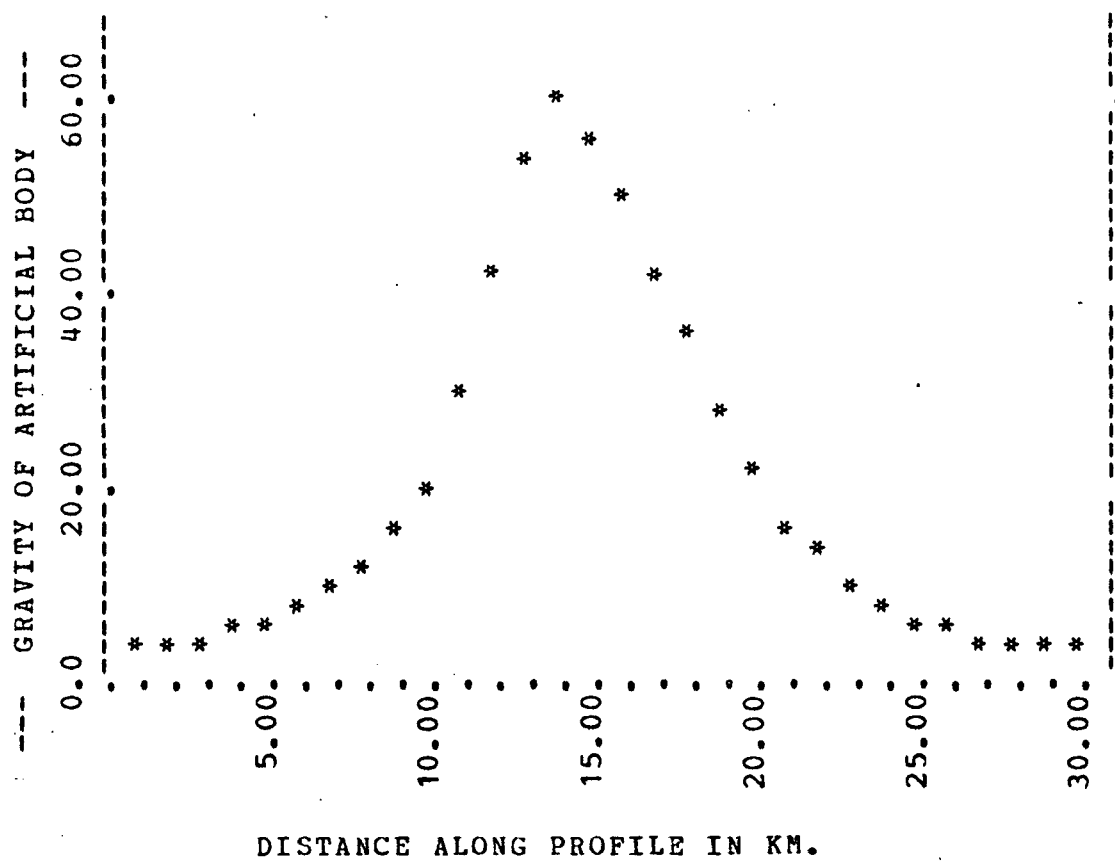
Fig. 11. Artificial gravity profiles used with the WEIGHT program.

--- GRAVITY OF ARTIFICIAL BODY ---

0.0   30.00   60.00   90.00   120.00   150.00

DISTANCE ALONG PROFILE IN KM.

5.00.

10.00.

15.00.

20.00.

25.00.

30.00.

z = 5.0

ρ = 1.0

(b)
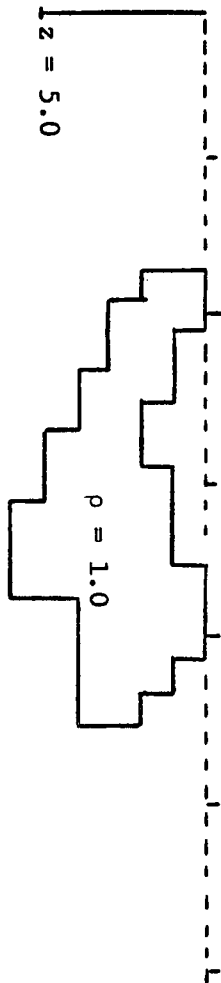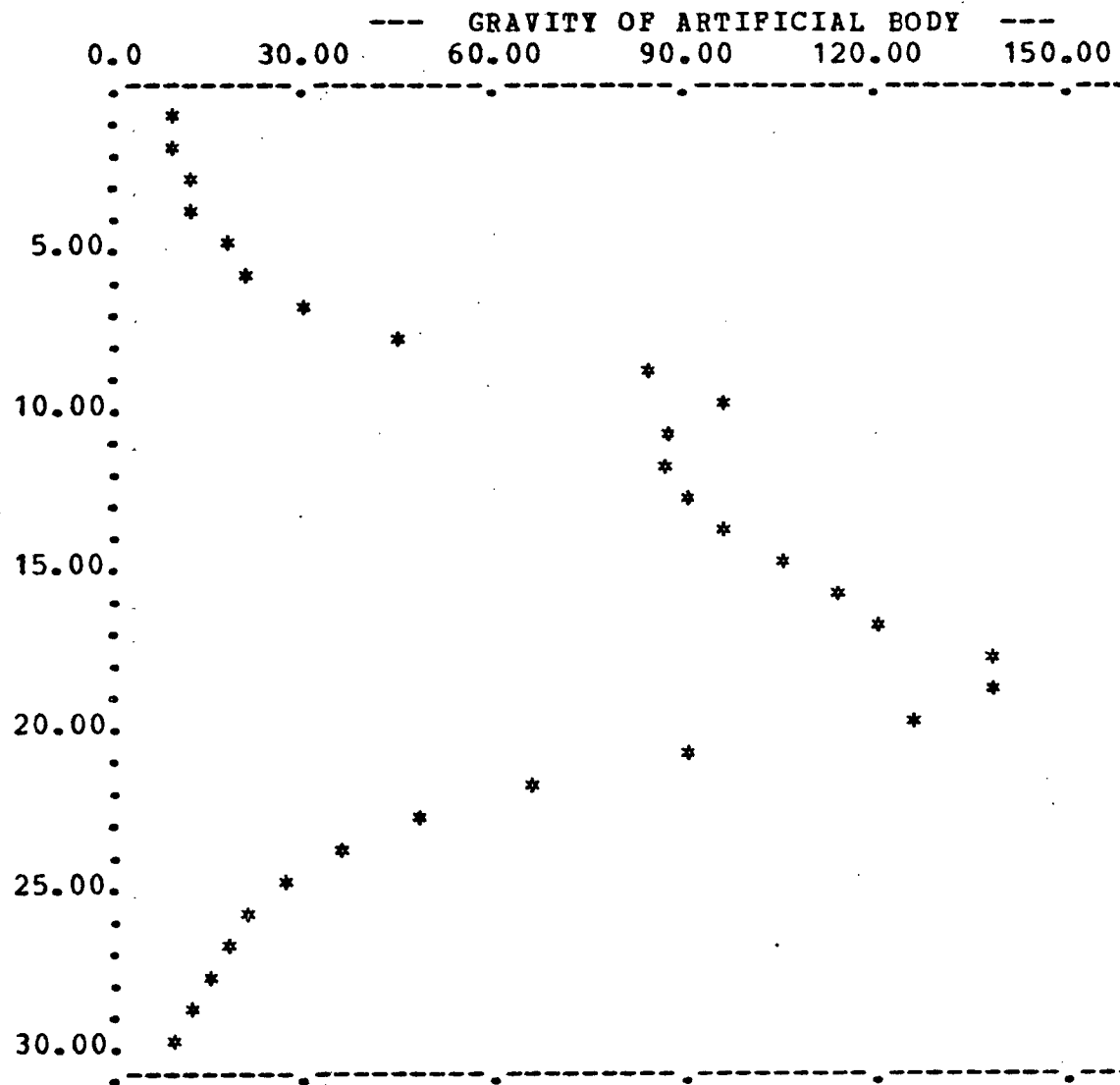
COMPUTED DENSITIES

X (KM) / Z=	0.50	1.50	2.50	3.50	4.50	5.50
7.00 :	-0.004	-0.005	-0.054	-0.008	-0.046	-0.118
8.00 :	-0.016	-0.005	-0.002	0.004	-0.010	-0.039
9.00 :	-0.029	0.013	0.036	0.045	0.043	0.034
10.00 :	-0.022	0.052	0.086	0.099	0.103	0.105
11.00 :	0.048	0.129	0.154	0.162	0.167	0.173
12.00 :	0.242	0.250	0.236	0.228	0.228	0.236
13.00 :	0.543	0.376	0.310	0.285	0.281	0.292
14.00 :	0.613	0.424	0.348	0.321	0.320	0.337
15.00 :	0.438	0.382	0.343	0.333	0.343	0.370
16.00 :	0.304	0.308	0.310	0.323	0.350	0.391
17.00 :	0.194	0.232	0.264	0.299	0.344	0.400
18.00 :	0.098	0.162	0.214	0.266	0.325	0.397
19.00 :	0.026	0.102	0.163	0.004	0.006	0.008
20.00 :	-0.015	0.056	0.113	0.172	0.244	0.343
21.00 :	-0.025	0.022	0.061	0.106	0.168	0.272
22.00 :	-0.015	-0.008	-0.001	0.031	0.045	0.141
23.00 :	-0.003	-0.003	-0.086	0.010	-0.182	-0.117

(a)   First result from a zero initial model.

INITIAL MODEL

X (KM) / Z=	0.50	1.50	2.50	3.50	4.50	5.50
10.00 :	0.0	0.0	0.0	0.0	0.0	0.0
11.00 :	0.0	0.0	0.0	0.0	0.0	0.0
12.00 :	0.0	0.0	0.0	0.0	0.0	0.0
13.00 :	0.0	0.800	0.800	0.800	0.0	0.0
14.00 :	0.0	0.800	0.800	0.800	0.0	0.0
15.00 :	0.0	0.0	0.800	0.800	0.800	0.0
16.00 :	0.0	0.0	0.0	0.800	0.800	0.0
17.00 :	0.0	0.0	0.0	0.800	0.800	0.800
18.00 :	0.0	0.0	0.0	0.0	0.800	0.800
19.00 :	0.0	0.0	0.0	0.0	0.800	0.0
20.00 :	0.0	0.0	0.0	0.0	0.0	0.0
21.00 :	0.0	0.0	0.0	0.0	0.0	0.0

(b)   A subsequent inversion's initial model.

Fig. 12.   Inversion of the profile in Figure 11(a).

APPROXIMATE DENSITIES

X (KM) / Z=	0.50	1.50	2.50	3.50	4.50	5.50
10.00 :	0.0	0.0	0.0	0.0	0.0	0.0
11.00 :	0.0	0.0	0.0	0.0	0.0	0.0
12.00 :	0.0	0.0	0.0	0.0	0.0	0.0
13.00 :	0.0	1.00	1.00	1.00	0.0	0.0
14.00 :	0.0	1.00	1.00	1.00	0.0	0.0
15.00 :	0.0	0.0	1.00	1.00	1.00	0.0
16.00 :	0.0	0.0	0.0	1.00	1.00	0.0
17.00 :	0.0	0.0	0.0	1.00	1.00	1.00
18.00 :	0.0	0.0	0.0	0.0	1.00	1.00
19.00 :	0.0	0.0	0.0	0.0	1.00	0.0
20.00 :	0.0	0.0	0.0	0.0	0.0	0.0
21.00 :	0.0	0.0	0.0	1.00	1.00	0.0

EXACT GRAVITY - APPROX GRAVITY - ERROR

	EXACT GRAVITY	APPROX GRAVITY	ERROR
1	3.1800	3.8327	-0.6527
2	3.6600	4.3786	-0.7186
3	4.2600	5.0502	-0.7902
4	5.0200	5.8894	-0.8694
5	6.0100	6.9565	-0.9465
6	7.3200	8.3422	-1.0222
7	9.1000	10.1855	-1.0855
8	11.6200	12.7081	-1.0881
9	15.3100	16.2755	-0.9655
10	20.8900	21.5070	-0.6171
11	29.3400	29.4415	-0.1015
12	41.2800	41.3973	-0.1173
13	54.0400	55.1149	-1.0749
14	59.1600	60.9357	-1.7757
15	55.5800	57.1730	-1.5930
16	49.5500	51.1622	-1.6123
17	42.5000	45.5201	-3.0201
18	35.0000	40.2489	-5.2489
19	27.9100	35.3689	-7.4589
20	21.8000	30.9025	-9.1025
21	16.9500	26.6177	-9.6677
22	13.2700	22.3314	-9.0614
23	10.5400	18.2792	-7.7392
24	8.5100	14.8068	-6.2968
25	6.9800	12.0270	-5.0470
26	5.8100	9.8659	-4.0559
27	4.9100	8.1947	-3.2847
28	4.1900	6.8935	-2.7035
29	3.6200	5.8688	-2.2488
30	3.1500	5.0511	-1.9011

(c) The approximate model obtained from (b).
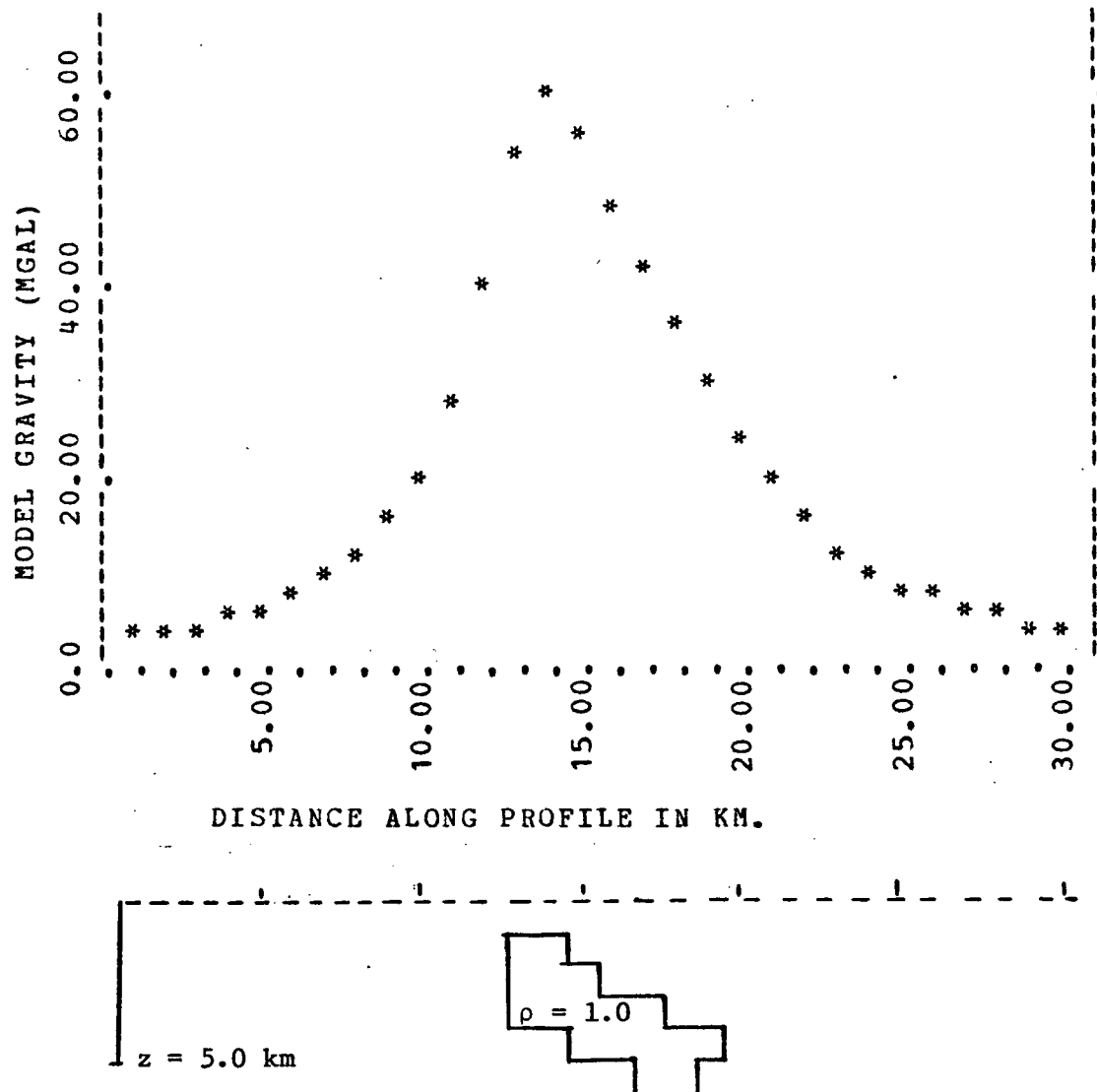
Fig. 13. A final model for the profile of Figure 11(a).

COMPUTED DENSITIES

X (KM) / Z=	0.50	1.50	2.50	3.50	4.50	5.50
6.00 :	-0.005	-0.159	0.047	-0.305	-0.254	-0.019
7.00 :	-0.073	0.021	0.058	0.000	0.017	0.125
8.00 :	-0.089	0.221	0.216	0.184	0.188	0.240
9.00 :	1.072	0.557	0.390	0.321	0.305	0.327
10.00 :	1.235	0.673	0.486	0.409	0.384	0.389
11.00 :	0.382	0.537	0.490	0.451	0.433	0.433
12.00 :	0.422	0.455	0.473	0.470	0.464	0.464
13.00 :	0.312	0.433	0.476	0.488	0.489	0.488
14.00 :	0.371	0.473	0.508	0.517	0.514	0.509
15.00 :	0.591	0.562	0.563	0.556	0.542	0.529
16.00 :	0.662	0.647	0.631	0.600	0.570	0.545
17.00 :	0.592	0.771	0.711	0.643	0.591	0.554
18.00 :	1.478	0.982	0.785	0.668	0.596	0.552
19.00 :	1.413	1.034	0.788	0.652	0.575	0.532
20.00 :	1.418	0.887	0.688	0.580	0.521	0.494
21.00 :	0.388	0.555	0.513	0.463	0.437	0.438
22.00 :	0.186	0.304	0.333	0.316	0.323	0.368
23.00 :	0.049	0.159	0.210	0.129	0.163	0.292
24.00 :	0.010	-0.005	0.294	-0.251	-0.096	0.237

APPROXIMATE DENSITIES

X (KM) / Z=	0.50	1.50	2.50	3.50	4.50	5.50
6.00 :	0.0	0.0	0.0	0.0	0.0	0.0
7.00 :	0.0	0.0	0.0	0.0	0.0	0.0
8.00 :	0.0	0.0	0.0	0.0	0.0	0.0
9.00 :	1.00	1.00	0.0	0.0	0.0	0.0
10.00 :	1.00	1.00	0.0	0.0	0.0	0.0
11.00 :	0.0	1.00	0.0	0.0	0.0	0.0
12.00 :	0.0	0.0	0.0	0.0	0.0	0.0
13.00 :	0.0	0.0	0.0	0.0	0.0	0.0
14.00 :	0.0	0.0	1.00	1.00	1.00	1.00
15.00 :	1.00	1.00	1.00	1.00	1.00	1.00
16.00 :	1.00	1.00	1.00	1.00	1.00	1.00
17.00 :	1.00	1.00	1.00	1.00	1.00	1.00
18.00 :	1.00	1.00	1.00	1.00	1.00	1.00
19.00 :	1.00	1.00	1.00	1.00	1.00	1.00
20.00 :	1.00	1.00	1.00	1.00	1.00	0.0
21.00 :	0.0	1.00	1.00	0.0	0.0	0.0
22.00 :	0.0	0.0	0.0	0.0	0.0	0.0
23.00 :	0.0	0.0	0.0	0.0	0.0	0.0
24.00 :	0.0	0.0	0.0	0.0	0.0	0.0

(a) First trial: initial model: $\rho = 0.5$ for all cells, uniform weighting.

Fig. 14. Inversion of the profile in Figure 11(b).

INITIAL MODEL

X (KM) / Z=	0.50	1.50	2.50	3.50	4.50	5.50
9.00 :	1.000	0.500	0.500	0.0	0.0	0.0
10.00 :	1.000	1.000	0.500	0.0	0.0	0.0
11.00 :	0.0	0.500	0.500	0.500	0.0	0.0
12.00 :	0.0	0.500	0.500	0.500	0.0	0.0
13.00 :	0.0	0.0	0.500	0.500	0.500	0.0
14.00 :	0.0	0.500	0.500	0.500	0.500	0.0
15.00 :	0.0	0.500	0.500	0.500	0.500	0.500
16.00 :	0.0	0.500	0.500	0.500	0.500	0.500
17.00 :	0.500	0.500	0.500	0.500	0.500	0.500
18.00 :	1.000	1.000	1.000	0.500	0.500	0.0
19.00 :	1.000	1.000	1.000	0.500	0.500	0.0
20.00 :	1.000	1.000	0.500	0.500	0.500	0.0
21.00 :	0.0	0.500	0.500	0.500	0.0	0.0
22.00 :	0.0	0.0	0.0	0.0	0.0	0.0

APPROXIMATE DENSITIES

X (KM) / Z=	0.50	1.50	2.50	3.50	4.50	5.50
9.00 :	1.00	1.00	0.0	0.0	0.0	0.0
10.00 :	1.00	1.00	1.00	0.0	0.0	0.0
11.00 :	0.0	1.00	1.00	1.00	0.0	0.0
12.00 :	0.0	1.00	1.00	1.00	0.0	0.0
13.00 :	0.0	0.0	1.00	1.00	1.00	0.0
14.00 :	0.0	1.00	1.00	1.00	1.00	0.0
15.00 :	0.0	1.00	1.00	1.00	1.00	1.00
16.00 :	0.0	1.00	1.00	1.00	1.00	1.00
17.00 :	0.0	1.00	1.00	1.00	1.00	1.00
18.00 :	1.00	1.00	1.00	1.00	1.00	0.0
19.00 :	1.00	1.00	1.00	1.00	1.00	0.0
20.00 :	1.00	1.00	1.00	1.00	1.00	0.0
21.00 :	0.0	1.00	1.00	1.00	0.0	0.0
22.00 :	0.0	0.0	1.00	1.00	0.0	0.0

(b) A subsequent inversion with an improved initial model.

```
WEIGHTED REGIONS
   X (KM) / Z=     0.50      1.50      2.50      3.50      4.50      5.50
......................................
       9.00  :     0.0       0.0       0.0       1.000     1.000     1.000
      10.00  :     0.0       0.0       0.0       0.0       1.000     1.000
      11.00  :     1.000     0.0       0.0       0.0       0.0       1.000
      12.00  :     1.000     0.0       0.0       0.0       0.0       0.0
      13.00  :     1.000     0.0       0.0       0.0       0.0       0.0
      14.00  :     1.000     0.0       0.0       0.0       0.0       0.0
      15.00  :     0.0       0.0       0.0       0.0       0.0       0.0
      16.00  :     0.0       0.0       0.0       0.0       0.0       0.0
      17.00  :     0.0       0.0       0.0       0.0       0.0       0.0
      18.00  :     0.0       0.0       0.0       0.0       0.0       0.0
      19.00  :     0.0       0.0       0.0       0.0       0.0       0.0
      20.00  :     0.0       0.0       0.0       0.0       0.0       0.0
      21.00  :     1.000     0.0       0.0       0.0       0.0       0.0
      22.00  :     1.000     1.000     0.0       0.0       0.0       0.0

THE WEIGHTING FACTOR IN CELLS MARKED 1.0 IS        50.0
THE WEIGHTING FACTOR IN CELLS MARKED 2.0 IS         1.0
THE WEIGHTING FACTOR IN CELLS MARKED 3.0 IS         1.0
OTHER REGIONS HAVE UNIT WEIGHT IN THE MINIMIZATION
```

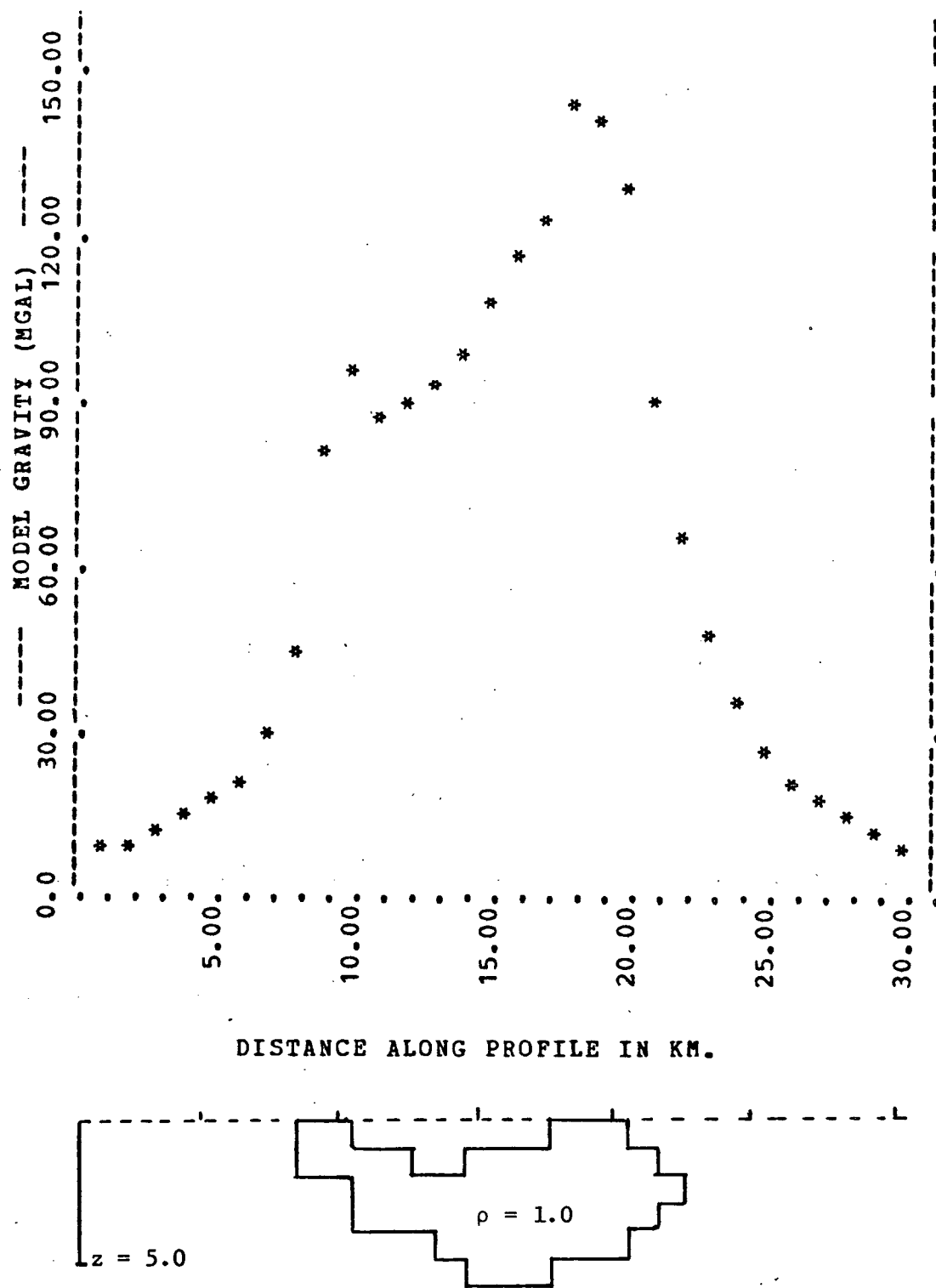(c) The weighting factors used in (b).

62

Fig. 15. Final model for the data of Figure 11(b).

data of Figure 11b. In this case, the final model was obtained in four iterations, and has a maximum error in gravity of about 6%.

These examples show that the weighted-distance method can quite readily produce acceptable models from artificial gravity data. The linear formulation allows several inversions to be made without requiring excessive computation time; the entire sequence of operations to produce the model in Figure 15 consumed about 40 seconds of CPU time on the IBM 360/67.

The ultimate aim of any inversion method is to produce models of the real earth, and thus the final test of the WEIGHT program was an inversion of gravity data taken over the Guichon Creek batholith in south central British Columbia. A detailed gravity survey was taken in 1971; other data were used as an aid in three-dimensional modelling (using a polygon method); and cross-sections were constructed from the complete model. The details of this work have been discussed by Ager (1972) and Ager et al (1972). The batholith is a long, narrow elliptical body, and thus should be amenable to two-dimensional modelling. The data treated by the new method were obtained from the Bouguer anomalies on one profile across the center of the batholith; a constant value could be substracted to satisfactorily remove the regional field (C. Ager, personal communication, 1973). The resulting gravity profile is shown in Figure 16.

Surface geological investigation indicates that the density contrast of the batholith is -0.15 gm/cm^3, and its surface outcrop extends for approximately 13 miles along the profile. From this information, the initial

DISTANCE ALONG PROFILE IN KM.
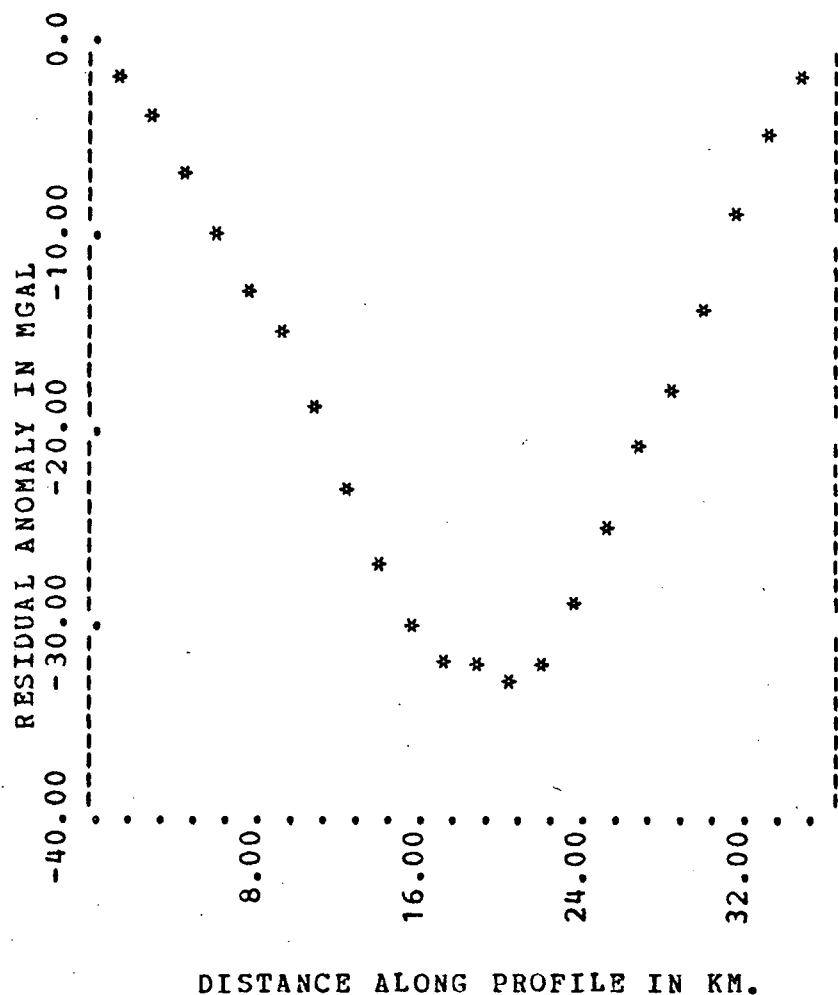
X	GZO
1.6	-2.1000
3.2	-4.1000
4.8	-6.9000
6.4	-9.8000
8.0	-12.7000
9.6	-15.5000
11.2	-18.7000
12.8	-22.9000
14.4	-27.5000
16.0	-30.5000
17.6	-31.6000
19.2	-32.2000
20.8	-32.7000
22.4	-32.0000
24.0	-29.4000
25.6	-25.3000
27.2	-21.2000
28.8	-17.6000
30.4	-13.7000
32.0	-9.2000
33.6	-5.0000
35.2	-1.9000

These values were obtained by subtracting -116 mgal from the Bouguer anomalies supplied by C. Ager.

(Note: his residual (Figure 19) was derived via a wavelength filtering method.)

Fig. 16. Residual anomaly over the Guichon Creek batholith.

model was chosen as a surface layer of density 0.15 in 13 cells (since the station spacing was one mile). The densities and the gravity data were considered to be positive, since the SMOOTH routine selects only positive densities in making approximate solutions (it could easily be adapted to treat either positive or negative density; the inversion itself does not depend on sign). To insure that the solution also had a surface density of 0.15, a weighting factor of 100.0 was applied to all the surface cells.

The approximate model obtained from the inversion is shown in Figure 17. There is a reasonable fit to the data; however the model is composed of three unconnected blocks, but a single anomalous body is expected. Three further applications of the program developed the single-body model shown in Figure 18. The shape indicated by the WEIGHT program inversions compares favourably with the cross-section obtained from a standard modelling method (Figure 19). It is evident that the new method can be successfully applied to real data.

One must be somewhat careful in applying the method to real data, for those data will not be perfectly accurate. In working with the batholith data, unrealistic inverses with large positive and negative densities often resulted from using models which did not span the entire region beneath the profile. The problem can be overcome by using a full-range model (i.e. the model's subsurface width equals the length of the profile), since the program can then assign small densities near any stations with erroneous data; rather than fitting the data by unrealistic density configurations beneath the center of the profile.

APPROXIMATE DENSITIES

X (KM) / Z=	0.80	2.40	4.00	5.60	7.20	8.80
1.60 :	0.0	0.0	0.0	0.0	0.0	0.0
3.20 :	0.0	0.0	0.0	0.0	0.0	0.0
4.80 :	0.0	0.0	0.0	0.0	0.0	0.0
6.40 :	0.0	0.15	0.0	0.0	0.0	0.0
8.00 :	0.0	0.30	0.0	0.0	0.0	0.0
9.60 :	0.15	0.0	0.0	0.0	0.0	0.0
11.20 :	0.15	0.0	0.0	0.0	0.0	0.0
12.80 :	0.15	0.0	0.0	0.0	0.0	0.0
14.40 :	0.15	0.15	0.15	0.15	0.0	0.0
16.00 :	0.15	0.15	0.15	0.15	0.15	0.0
17.60 :	0.15	0.15	0.15	0.15	0.15	0.0
19.20 :	0.15	0.15	0.15	0.15	0.15	0.0
20.80 :	0.15	0.15	0.15	0.15	0.15	0.0
22.40 :	0.15	0.15	0.15	0.15	0.15	0.0
24.00 :	0.15	0.15	0.15	0.15	0.0	0.0
25.60 :	0.15	0.15	0.0	0.0	0.0	0.0
27.20 :	0.15	0.0	0.0	0.0	0.0	0.0
28.80 :	0.15	0.0	0.0	0.0	0.0	0.0
30.40 :	0.0	0.30	0.15	0.0	0.0	0.0
32.00 :	0.0	0.15	0.0	0.0	0.0	0.0
33.60 :	0.0	0.0	0.0	0.0	0.0	0.0
35.20 :	0.0	0.0	0.0	0.0	0.0	0.0

EXACT GRAVITY - APPROX GRAVITY - ERROR

1	2.1000	3.2526	-1.1526
2	4.1000	4.4243	-0.3243
3	6.9000	6.5287	0.3713
4	9.8000	9.7191	0.0809
5	12.7000	12.6765	0.0235
6	15.5000	17.7263	-2.2263
7	18.7000	19.5345	-0.8345
8	22.9000	22.5727	0.3273
9	27.5000	26.7013	0.7987
10	30.5000	29.9065	0.5935
11	31.6000	31.7112	-0.1112
12	32.2000	32.3741	-0.1741
13	32.7000	32.0374	0.6626
14	32.0000	30.7138	1.2862
15	29.4000	28.3698	1.0302
16	25.3000	25.0967	0.2033
17	21.2000	21.6822	-0.4822
18	17.6000	19.5061	-1.9061
19	13.7000	14.3055	-0.6055
20	9.2000	11.0188	-1.8188
21	5.0000	7.4272	-2.4272
22	1.9000	5.0234	-3.1234

Fig. 17. The first inversion of the batholith anomaly.
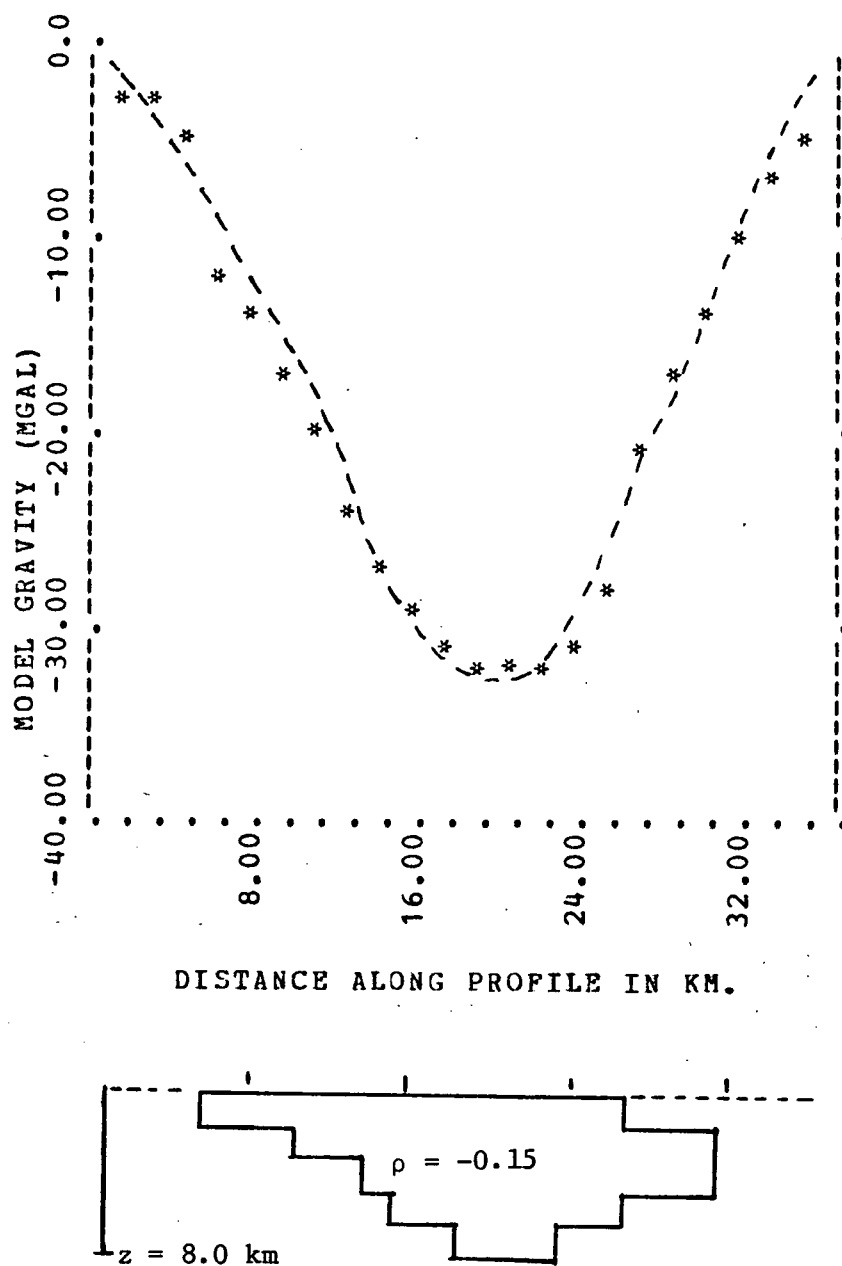
The dashed line indicates the residual anomaly of Figure 16.

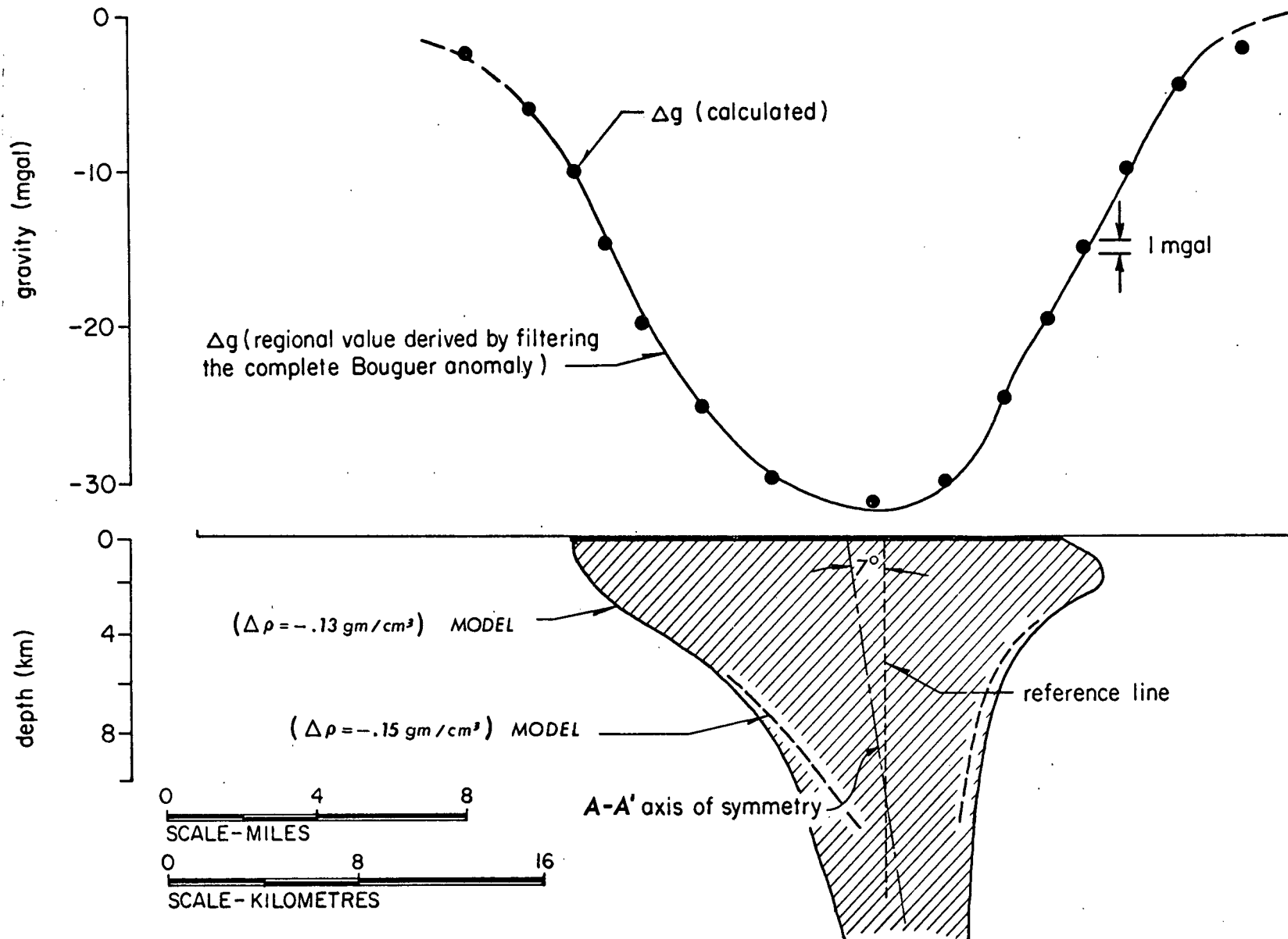Fig. 18. A model for the Guichon Creek batholith.

Fig. 19. A batholith cross-section obtained by standard modelling methods (from Ager et al, 1972).

In conclusion, it is suggested that the models produced by a "weighted-distance" minimization are a reasonable means of interpreting gravity data. Artificial data for two simple bodies, as well as a real gravity profile, have been inverted by successive applications of the WEIGHT program; in each case a simple model of one density was obtained. The process is not completely objective, since improvement of initial models is at the discretion of the interpreter. However, the linear functionals allow rapid computation of each inverse, so the method can be applied several times at a modest cost in computer time.

CHAPTER 5

Numerical Optimization Of Gravity Models Using Entropy

5.1 Entropy of Gravity Models

It was noted earlier that gravity interpretation often has the objective of defining the shape of a body of anomalous density. If the inversion technique uses a combination of simple bodies, a method to find a compact grouping of those units is desirable. To produce such single-density models from Backus-Gilbert inversions, it is usually necessary to apply considerable interpretive judgement. In hopes of developing a more objective method for finding compact models, we can investigate criteria for selecting an acceptable model of the desired form. In particular, the concept of an entropy assigned to a density model will be applied as a measure of "order" or "structure" of the model, following a suggestion of G.K.C. Clarke (personal communication, 1971).

Entropy concepts are used in many areas of physics and mathematics, and the success of entropy methods in other fields led to the present investigation. In statistical mechanics, the entropy of a closed system is

$$H = - \Sigma \; p_s \; \log \; p_s$$

where p_s is the probability that the system is in state s. In general, maximum entropy corresponds to the equilibrium state (Kittel, 1958). Information theory uses entropy as a measure of average information (or average uncertainty) of a message source (Lathi, 1968). In spectral analysis, the maximum entropy method developed by Burg (1967) has been quite successful, particularly in resolving frequency components from short records (Lacoss, 1971; Ulrych, 1972)

Clarke's suggestion for using entropy of a density model differs from the usual applications, since minimum entropy will be sought as a criterion of maximum order of the model. In this sense, the idea is another method for selecting a particular model from all those which satisfy the gravity data.

Minimum entropy is an apparent conflict with the principles of statistical mechanics and thermodynamics, since the equilibrium state of any system should have maximum entropy. Nevertheless, minimum entropy can be a useful property, if it can produce the most structured model compatible with the data, since structures or concentrated bodies are the usual target of geophysical exploration. In addition, the maximum entropy principle in physical systems is not inviolable. Fast (1968) observed that in some substitutional alloys, the tendencies toward entropy maximization and energy minimization conflict. Prigogine et al (1972) examined development of biological ordered systems, and concluded that fluctuations in irreversible systems could produce low entropy configurations, which need not be the lowest probability state of the system. In light of these examples, it is reasonable to look for minimum entropy models, without being concerned that they may be physically improbable if the crustal density distribution is a random process. The knowledge that compact ore bodies do exist in the earth's crust in itself supports the argument.

By analogy with other applications, the entropy of a density model is defined by

$$H = - \int_V \frac{\rho}{M} \ln \frac{\rho}{M} \, dV \tag{1}$$

The normalized variable $\frac{\rho}{M}$ is used to give the appearance of a probability density function, which requires

$$\int_V \frac{\rho}{M} \, dV = 1$$

$$0 < \frac{\rho}{M} < 1$$

$$\int \frac{\rho}{M} \, dV \text{ is monotonically increasing}$$

For the linear density models, (1) becomes

$$H = - \sum_n \sum_m \frac{\rho_{nm}}{M} \ln \frac{\rho_{nm}}{M} \tag{2}$$

where

$$M = \sum_n \sum_m \rho_{nm} \qquad \text{(cell dimensions cancel in (2))}$$

To find the desired compact or structured model, (2) must be minimized under the constraints imposed by the known gravity anomaly. In the present formulation, these are

$$\sum_n \sum_m G_{jnm} \, \rho_{nm} = g_j = \lambda_j \tag{3}$$

In addition, bounds can be imposed on density to produce geologically reason-

able models. We also require ρ to have the same sign everywhere, if $\frac{\rho}{M}$ is

to have the properties of probability. The additional constraints are now

expressed as

$$0 \leqslant \rho_{nm} \leqslant A \tag{4}$$

(or opposite signs for a negative anomaly).

To find a method to solve this problem, we first examine the

properties of entropy in density models. A decrease in entropy as models

become more compact is confirmed by considering horizontal cylinders of

different density but equal mass. Such cylinders will produce the same

gravity profile if centered at the same depth. To compute the entropy of

these simple models, (1) is simplified by considering density to be constant

inside the cylinder. Since the cylinder mass M is constant $\frac{\rho}{M} = \frac{1}{V}$ is

constant for a given cylinder (V is the volume). Then

$$H = - \int_V (\frac{1}{V}) \ln (\frac{1}{V}) \, dV = \ln V = - \ln \frac{\rho}{M} \tag{5}$$

Since $\quad \lim_{x \to 0} x \ln(X) = 0,$

integration is done only over the cylinder. For the two-dimensional models,

V is actually the cross-sectional area. The variation of entropy with the

density and radius of the cylinder is shown in Figure 20; we consider cylin-

ders of different density as acceptable models for the same gravity profile.

The entropy minimum will correspond to a point mass (radius $\to$ 0), and the

maximum to a cylinder of infinite radius ($\rho \to 0$).

Fig. 20. Entropy of horizontal cylinders of equal mass.

Figure 20 demonstrates that entropy has an absolute minimum only

in the limiting sense of the model becoming a point mass. We require bounds

on density (as in equation (4)), and thus entropy minimization must be done

in a bounded density interval. A major problem is that the minimum is not

a stationary point (i.e. we do not have $\frac{\partial H}{\partial \rho} = 0$) and thus the classical mini-

mization procedures cannot be used. The upper bound on density, A, should

be chosen as the desired density of the final model, since (5) implies that

the minimum entropy model will have the least possible volume. Minimizing

entropy of the linear models should then assign a density of zero or A to

each prism; hence a constant density model would be produced.

Another consequence of equation (5) is that model entropy is a

useful property only if density is a variable parameter. Any model which

assumes constant density also has constant entropy, since the mass is a

known constant; i.e. by specifying the density of a model, one is also

specifying its entropy.

5.2 Numerical Optimizations of Model Entropy

Minimizing entropy under the constraints (3) and (4) is a dif-

ficult non-linear optimization problem, which cannot be solved by the tech-

niques of variational calculus, since the minimum is not a stationary point.

As a result, a somewhat different viewpoint of the model is developed; we

consider the densities of N prisms as N independent parameters, rather than

viewing density as a single parameter which varies with the spatial coor-

dinates. The problem is then an optimization in an N-dimensional space.

There are many methods for optimization in general parameter spaces, but

most are designed for specialized problems, so that a particular example is often tractable with only one or two procedures. Beveridge and Schechter (1970) have analyzed many numerical methods and discussed their feasibility for various problems. On their recommendation, and that of the UBC Computing Center (C. Bird, personal communication, 1973), the COMPLEX search method of Box (1965; Box et al 1969) was adapted to minimize entropy.

The major advantage of the COMPLEX method for the entropy problem is that it makes no use of derivatives or gradients. Derivatives of model entropy cannot be used, since they become infinite for those cells whose density approaches zero, and the desired compact models will have prisms of zero density.

$$H = - \Sigma \frac{\rho}{M} \ln \frac{\rho}{M} = - \Sigma \rho' \ln \rho'$$

$$\frac{\partial H}{\partial \rho'} = \frac{\rho}{\partial \rho} (\rho' \ln \rho') = \ln \rho' + 1 \tag{6}$$

$$\text{and} \quad \lim_{\rho' \to 0} \ln \rho' = - \infty$$

This difficulty led to the rejection of most popular optimization methods. A brief description of the general ideas behind these techniques is given in Appendix D.

The COMPLEX method follows an initial strategy somewhat similar to Monte Carlo modelling. Starting with one acceptable model (considered to be a point in the N-dimensional parameter space), a set of "points" with

random coordinates are generated. The random points can be made to define
new acceptable models (or "feasible points") by moving them towards the
centroid of feasible points until all constraints are satisfied. The
feasible points define the vertices of a figure termed a "complex". Searching
for the optimum of an objective function consists of evaluating the function
at each vertex, rejecting the vertex of "worst" value, and replacing it by
reflection through the centroid of remaining points. At each step, tests
are required to make sure each new point is feasible; in addition, additional
strategies can be employed to keep the search moving towards the optimum
point. The details of the method, along with modifications developed for
the present use, are described in Appendix E.

The application of a COMPLEX search to the minimum entropy problem
is quite straightforward. The coordinates of the parameter space are the
densities of the N prisms which comprise the model. All densities are
assumed to lie in the interval [0,A], where A is the expected constant
density of an anomalous body. The implicit constraints are a known gravity
anomaly, λ_j, which must be satisfied within a specified limit δ; thus the
constraints are written

$$\left| \lambda_j - \sum_n \sum_m G_{jnm} \rho_{nm} \right| \leqslant \delta \qquad\qquad \text{or}$$

$$-\delta \leqslant \left(\lambda_j - \sum_n \sum_m G_{jnm} \rho_{nm} \right) \leqslant \delta \qquad\qquad (7)$$

along with the bounds

$$0 \leqslant \rho_{nm} \leqslant A \qquad\qquad (8)$$

Equations (7) and (8) are linear in ρ_{nm}, and thus the feasible region is

convex, since it can be shown that any region whose boundaries are defined

by linear constraints is convex (Beveridge and Schechter, 1970, p. 113;

Cooper and Steinberg, 1970, p. 68).

It is convenient to write the necessary computer programs in

several parts; the programs used here were as follows. The START program

computes all necessary arrays (such as the Frechet kernels) and passes

them, along with an acceptable model and the gravity data, to the searching

routines. POINTS generates the initial complex from the starting model.

The TEST subroutine ensures that each point satisfies the implicit constraints

(7). SEARCH does the rest of the job, computing entropies, finding "worst"

points, and generating new ones. The optional routine RESTAR (very similar

to POINTS) will create a new complex from the current best point if: (a)

the centroid appears to be unfeasible; (b) the search is stalled at one

vertex; or (c) a specified number of iterations have been completed.

Several subtle difficulties can arise in obtaining reasonable

results from these programs. Since the search region is convex, the centroid

of feasible points must always lie within it; however the finite precision

of the computer may cause an apparently unfeasible centroid when the search

is near a boundary. This problem can usually be overcome by generating a

new complex from the current best point. To maintain a reasonable rate of

progress, a fairly generous error should be permitted in applying the con-

straints; a general rule of thumb is to set δ at 5% to 10% of the maximum

gravity. The limits of model gravity allow acceptable models to have a range

of masses; frquently the search will initially only reduce the mass before concentrating it in as few cells as possible. In these cases, the final model tends to have a smaller mass than is indicated by the data; the densities could be multiplied by an appropriate scale factor to restore the true mass.

The first test of the method was a simple example to show that the minimum entropy model will in fact be the most compact. A simple 9-prism model was used, with gravity constraints generated by a density of 0.9 in the center cell. The search started from a model with mass 0.5 in the central block, and 0.4 distributed around it, as shown in Figure 21. As expected, entropy minimization concentrated all the mass in the center block.

A more difficult problem is to start from a very diffuse initial model; in the previous example, the center cell was clearly dominant in the initial model. This time a 12-parameter model was used, with gravity data generated by a unit-density cell in the third block of the middle column. The initial model had density 0.11 in the nine cells grouped around the expected source of the anomaly. This search did not successfully converge, as the cells whose mass initially increased were not in the central location. The model obtained in 600 iterations is shown in Figure 22. It seems likely that a very diffuse initial model may be brought to an intermediate stage of compactness which cannot be further improved.

To test the method on a possible exploration objective, the gravity profile of the body shown in Figure 23 was used. A starting point was ob-

```
INITIAL MODEL

Z (KM)/ X=      14.00     15.00     16.00
             ...................................

      1.50 :     0.050     0.050     0.050

      2.50 :     0.050     0.500     0.050

      3.50 :     0.050     0.050     0.050


         TOTAL MASS IS          0.9000
         MODEL - ENTROPY

              1      1.61116
```

    15 FEASIBLE POINTS WILL BE PICKED
    400 IS THE MAXIMUM NUMBER OF ITERATIONS ALLOWED
A NEW COMPLEX WILL BE GENERATED EVERY 125 ITERATIONS
NO RESTARTING OF THE COMPLEX AFTER   5 ITERATIONS
THE GRAVITY WILL AGREE WITHIN 0.400 MGAL
UPPER DENSITY LIMIT IS 1.00 GM/CC
CONVERGENCE IF CENTROID ENTROPY AGREES WITHIN 0.10E-05
THE RANDOM NUMBER GENERATOR IS INITIALIZED AT 0.0
THE EXPANSION PARAMETER OF THE COMPLEX IS 1.40

        CONVERGENCE WITHIN SPECIFIED LIMIT:

```
FEASIBLE POINT NO.      9
 Z (KM)/ X=      14.00     15.00     16.00
             ...............................

      1.50 :     0.002     0.001     0.002

      2.50 :     0.000     0.951     0.001

      3.50 :     0.001     0.001     0.000


      CENTROID ENTROPY=       0.0001397

      CENTROID MASS=          0.9590
```
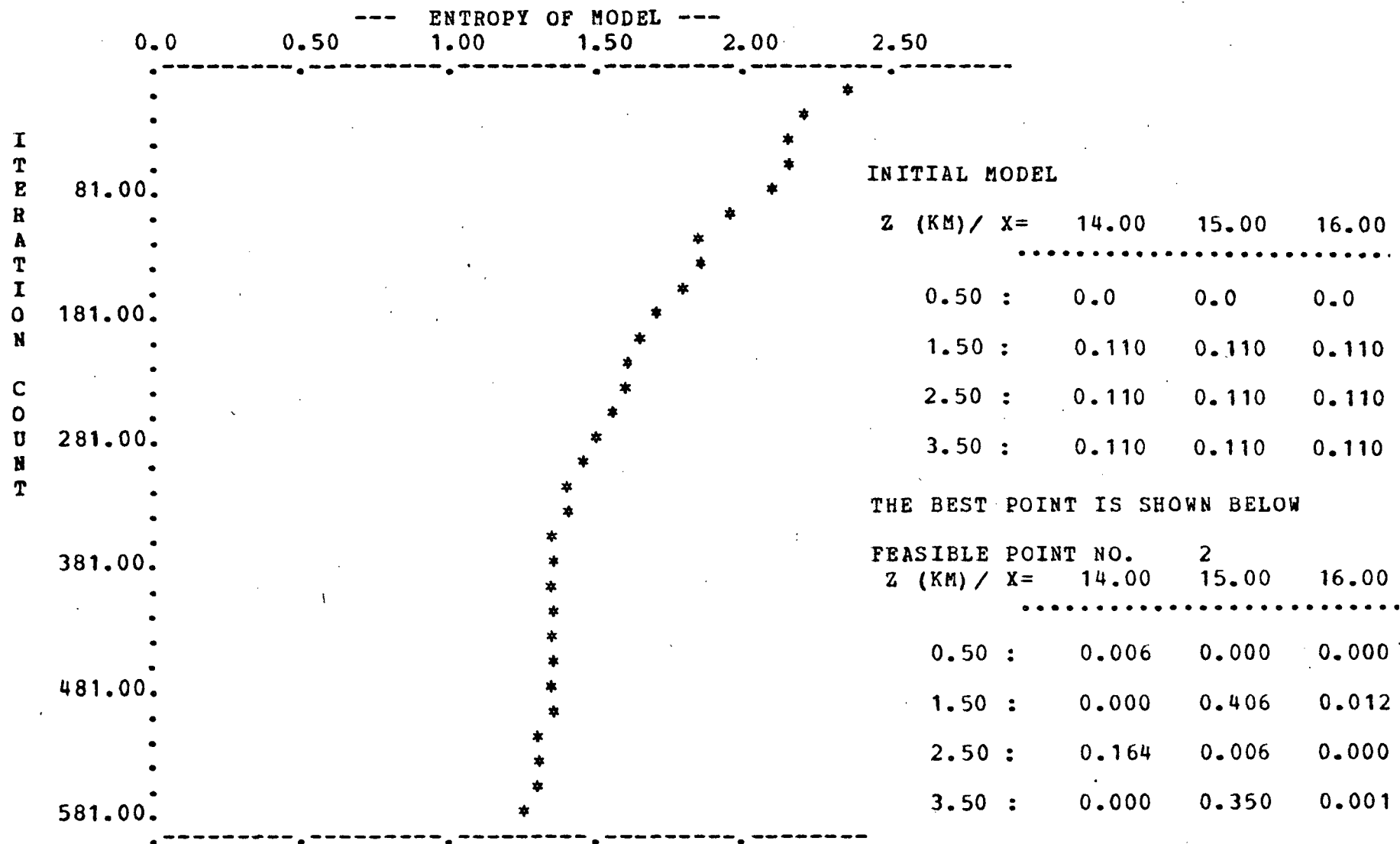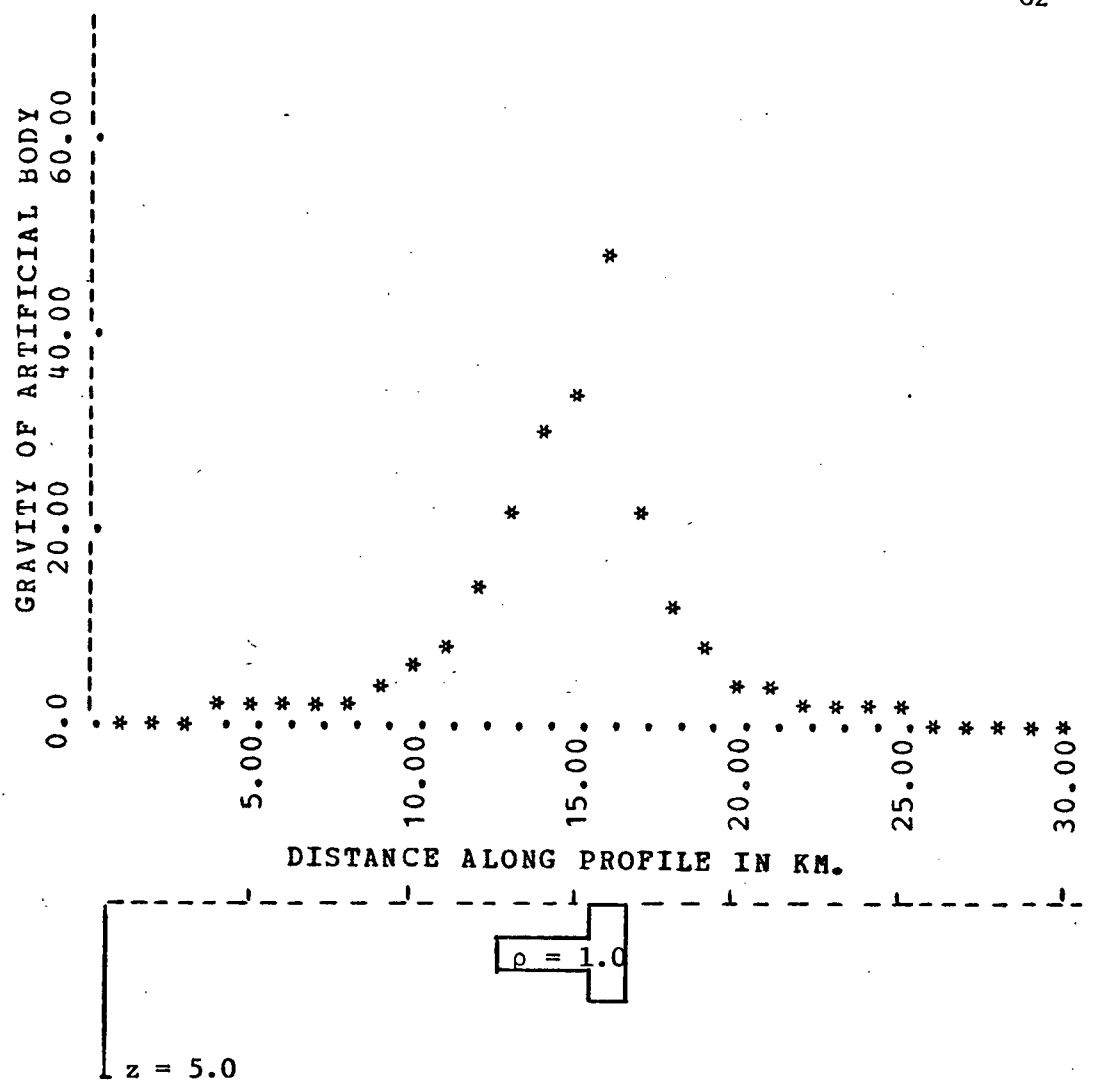
Fig. 21. A simple entropy minimization.

Fig. 22.   Minimum entropy from a diffuse starting model.

GRAVITY OF ARTIFICIAL BODY

DISTANCE ALONG PROFILE IN KM.

ρ = 1.0

z = 5.0

Computer Display

Z (KM)/ X=	13.00	14.00	15.00	16.00
0.50 :	0.0	0.0	0.0	1.000
1.50 :	1.000	1.000	1.000	1.000
2.50 :	0.0	0.0	0.0	1.000

Fig. 23. An artificial gravity profile for entropy minimization.

INITIAL MODEL

Z (KM)/ X=	12.00	13.00	14.00	15.00	16.00	17.00	18.00
0.50 :	0.0	0.100	0.200	0.200	1.000	0.100	0.0
1.50 :	0.100	0.400	0.400	0.500	0.800	0.100	0.200
2.50 :	0.0	0.400	0.700	0.700	0.300	0.0	0.0

TOTAL MASS IS   6.2000   MODEL - ENTROPY

1   2.52968

THE BEST POINT IS SHOWN BELOW

FEASIBLE POINT NO.   18

Z (KM)/ X=	12.00	13.00	14.00	15.00	16.00	17.00	18.00
0.50 :	0.000	0.002	0.000	0.000	0.994	0.002	0.000
1.50 :	0.000	0.000	0.675	0.766	0.988	0.000	0.001
2.50 :	0.002	0.586	0.998	0.942	0.002	0.000	0.017

CENTROID ENTROPY=   1.9187727

CENTROID MASS=   5.9904

Model gravity accurate within 3.0 mgal.

Fig. 24.   A minimum entropy model from the artificial profile.

tained by using a "zero" initial model in the WEIGHT program of Chapter 4. The results of this example are shown in Figure 24; the allowed error has permitted a solution different from the "real" body. The final solution also seems to reflect the starting model, since the largest densities of that model were all increased. Nonetheless, the method is partially fulfilling our basic purpose; to provide an objective means for producing a compact model from the diffuse inversions produced by the methods of Chapter 4.

One advantage of the COMPLEX method is that it can easily optimize different objective functions. A simple function which may also produce a final model of density A is

$$F(\rho) = - \Sigma \Sigma \rho_{nm} (\rho_{nm} - A) \qquad (9)$$
$$ n \; m$$

Each term in the summation is zero at $\rho=0$ and $\rho=A$, hence minimizing $F(\rho)$ should set each ρ_{nm} to a value of 0 or A. The similarity to entropy is illustrated in Figure 25. This is to be expected, since the first term in a Taylor series for $\ln(x)$ is $(x-1)$ (Abramowitz and Stegun, 1965, p. 68), and thus the first term in $(x) \ln(x)$ is $x(x-1)$. The main difference is that $F(\rho)$ is not normalized, which can be an advantage in the minimization, particularly if the mass of the model is greater than about 3.0 (here mass refers to the sum of all prism densities, as in Equation (2)). In such cases, the contribution to entropy from each cell is restricted to the interval $x<0.3$ in Figure 25; and an increase in density for any cell will not improve the objective function. In minimizing the unnormalized function (9), bringing an individual density towards A will still improve the value
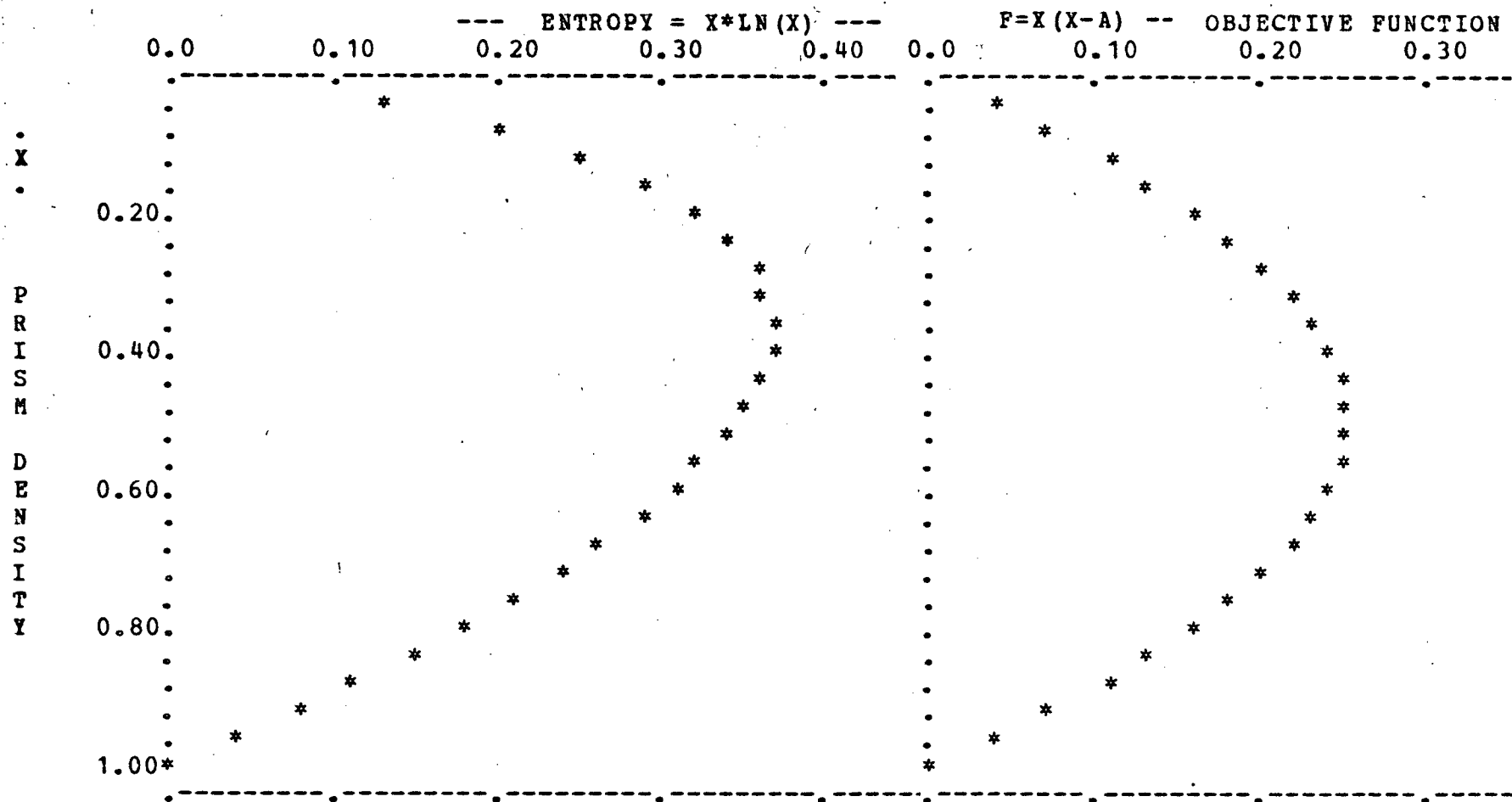
Fig. 25.   The functions x ln(x) and x(x-A).

INITIAL MODEL

Z (KM)/ X=	12.00	13.00	14.00	15.00	16.00	17.00	18.00
0.50 :	0.0	0.100	0.200	0.200	1.000	0.100	0.0
1.50 :	0.100	0.400	0.400	0.500	0.800	0.100	0.200
2.50 :	0.0	0.400	0.700	0.700	0.300	0.0	0.0

TOTAL MASS IS   6.2000   OBJECTIVE FUNCTION 2.59999

THE BEST POINT IS SHOWN BELOW

Z (KM)/ X=	12.00	13.00	14.00	15.00	16.00	17.00	18.00
0.50 :	0.0	0.0	0.001	0.0	0.989	0.0	0.0
1.50 :	0.004	0.997	0.0	0.996	0.996	0.0	0.0
2.50 :	0.0	0.845	0.998	0.138	0.001	0.029	0.001

MASS IS   5.9950   CENTROID FUNCTION=   0.3207084

Model gravity accurate within 3.0 mgal

Fig. 26. An optimum model for Figure 23, using x(x-A).

of the objective function.

The new function can be optimized with the same basic programs, except that the SEARCH routine no longer computes entropies. The example of Figure 24 was repeated, with results shown in Figure 26. In the same number of iterations, $F(\rho)$ has been more successful than entropy in putting all the mass in cells of density A, which is probably a result of entropy being normalized by a mass M=6.0. Once again the error limit has prevented exact duplication of the body in Figure 23. This example suggests that $F(\rho)$ is a reasonable alternative to entropy, particularly for multi-block models; however the nature of the search will likely prohibit any dramatic saving of computer time.

The optimization programs can also be easily adapted to find maximum entropy models, which may be of interest if maximum entropy does indicate the most probable state (although it may be suggested that the most probable density configurations preclude the existence of gravity anomalies). By analogy to the arguments suggesting minimum entropy as a measure of compactness, maximum entropy should produce the most diffuse model compatible with the observations.

Maximum entropy models were computed for two of the earlier examples for direct comparison to minimum entropy. Figure 27 is the result of 400 iterations of the simple 9-parameter model; the maximization is clearly trying to evenly distribute the mass. Figure 28 is the comparison for the gravity profile of Figure 23. Maximizing entropy has not made any

INITIAL MODEL

Z (KM)/ X=	14.00	15.00	16.00
1.50 :	0.050	0.050	0.050
2.50 :	0.050	0.500	0.050
3.50 :	0.050	0.050	0.050

TOTAL MASS IS   0.9000

MODEL - ENTROPY

1   1.61116

THE BEST POINT IS SHOWN BELOW

FEASIBLE POINT NO.   13

Z (KM)/ X=	14.00	15.00	16.00
1.50 :	0.100	0.040	0.077
2.50 :	0.029	0.228	0.091
3.50 :	0.143	0.232	0.103

CENTROID ENTROPY=   2.1702032

CENTROID MASS=   1.0422

Model gravity accurate within 0.4 mgal.

Fig. 27. A maximum entropy model corresponding to Figure 21.

Z (KM)/ X=	12.00	13.00	14.00	15.00	16.00	17.00	18.00
0.50 :	0.000	0.002	0.000	0.000	0.994	0.002	0.000
1.50 :	0.000	0.000	0.675	0.766	0.988	0.000	0.001
2.50 :	0.002	0.586	0.998	0.942	0.002	0.000	0.017

(a) Minimum entropy.

Z (KM)/ X=	12.00	13.00	14.00	15.00	16.00	17.00	18.00
0.50 :	0.001	0.128	0.217	0.261	0.946	0.135	0.017
1.50 :	0.187	0.473	0.401	0.591	0.561	0.149	0.239
2.50 :	0.281	0.493	0.674	0.532	0.258	0.125	0.109

(b) Maximum entropy.

Fig. 28. A comparison of maximum and minimum entropy models for Figure 23.

N	K	ITMAX	CPU TIME (sec.)	COMMENTS
9	15	400	34	converged
12	15	600	58	partly converged
18	21	400	61	partly converged
21	25	500	82	partly converged
60	62	1000	501	no progress

N = Number of parameters

K = Number of points in the complex

ITMAX = Number of iterations

TABLE IV. Computation time for numerical optimizations.

dramatic change in the model, while minimum entropy has had some success in concentrating the mass. Our expectations regarding maximum entropy models seem to be upheld.

The numerical optimizations were not successful in developing any really complex models, largely because they require very extensive computations. Table IV shows the CPU time consumed for various trials of the minimum entropy program. The 60-parameter example was an attempt to improve a simple model for the artificial profile of Figure 11a, Chapter 4 (the initial model was obtained using the WEIGHT program); there was no discernible improvement towards compactness in 1000 iterations. We conclude that the numerical method is not practical for any excessive number of parameters (i.e. prisms in the model).

The results of numerical optimizations support the suggestion that minimizing entropy will produce a compact model, i.e. a model of maximum allowable density. Simpler objective functions can also be adopted towards the same goal. Unfortunately, the straightforward application of these criteria is very time-consuming. It appears that these optimum models, as presently derived, are not practical for any complex system requiring many parameters. However, this does not necessarily mean that a practical minimum entropy method cannot be developed; since there may be many other approaches to the problem, for example transformation into a space where entropy is a more simply-behaved function.

CHAPTER 6

Conclusion

Geophysicists are continually seeking new ways to obtain accurate data and extract information from them. In many applications, modelling plays an integral role in interpretation. Gravity exploration data lend themselves to modelling techniques, and it is hoped that some of the new developments for gravity problems presented here can be useful in exploration situations.

The linear models proposed in Chapter 3 have proven quite useful for inverting gravity profiles via a Backus-Gilbert approach (developed in Chapter 4). Initial experience with the "weighted-distance" method indicates that it is flexible, particularly in iterative use, when certain densities from the previous solution can be held constant. Approximate models (composed of prisms of a single density) can frequently give an adequate fit to a given profile after 4 or 5 repetitions, at quite modest expense in terms of computer time.

Reasonable care must be taken with real data to ensure an acceptable solution. It is perhaps best to use models spanning the subsurface region beneath the profile, so that the inversion can more easily account for noise in the data. If a model has too few prisms to adequately represent the data, an oscillatory solution (i.e. large positive and negative densities) may result.

There are many possibilities for further improvement of the methods of Chapter 4. The present work certainly justifies more application to real

data. In some situations, it appears that the requirement of exact agreement with the data is detrimental; the inversion produces an exceptionally close fit by using unrealistic densities. In these examples, it may be helpful to relax the constraints, by demanding agreement only within a specified error. Gilbert (1971) and Wiggins (1972) have discussed ways in which this might be achieved.

The large-block models may also prove useful for real data, if the problem of bad solutions for high-frequency data can be overcome. It may be possible to find acceptable inverses in the spatial frequency domain, and fit the model only to the lower frequency components of the data. The large blocks could then be subdivided for further improvement using the complete data set.

The investigation of entropy in Chapter 5 demonstrates that optimizing a compactness property of a density model is a feasible idea, although not necessarily a practical one. Other approaches to the entropy problem may well be more efficient. Numerical optimization was of some help in solving a difficult problem, and might conceivably be useful with many other types of models.

The COMPLEX method described in Chapter 5 might be easily adapted to other problems if three simple changes are made: (1) allow a variable number of constraints (the present program requires 30); (2) incorporate objective function evaluations as a separate routine; and (3) add an indicator to choose maximization or minimization. It appears that the COMPLEX method will work best with a small number of parameters, so the large-block models might be of some benefit here.

All the investigations herein were pursued in hopes of gaining some basic insight into the nature of the modelling process. Perhaps the greatest benefit from these studies is the knowledge that new methods from other areas of geophysics and applied mathematics can easily be adapted to the problems of exploration geophysics.

REFERENCES

Abramowitz, M., and I. Stegun, 1965, Handbook of Mathematical Functions, Dover, New York.

Agarwal, B.N.P., 1971, Direct gravity interpretation of sedimentary basin using digital computer, Part I and II, Pure Appl. Geophys. v. 86, pp. 5-17.

Ager, C.A., 1972, A gravity model for the Guichon Creek batholith, unpublished M.Sc. thesis, University of B.C.

Ager, C.A., W.J. MacMillan, and T.J. Ulrych, 1972, Gravity, magnetics and geology of the Guichon Creek batholith, Bulletin 62, B.C. Dep't of Mines and Petroleum Resources.

Al-Chalabi, M., 1971, Some studies relating to nonuniqueness in gravity and magnetic inverse problems, Geophysics, v. 36, pp. 835-855.

------, 1972, Interpretation of gravity anomalies by non-linear optimisation, Geophys. Prosp., v. 20, pp. 1-16.

Anderssen, R.S., 1970, The character of non-uniqueness in the conductivity modelling problem for the earth, Pure Appl. Geophys., v. 80, pp. 238-259.

Anderssen, R.S., M.H. Worthington, and J.R. Cleary, 1972, Density modelling by Monte Carlo inversion, I - Methodology, II - Comparison of recent earth models, Geophys. J., v. 29, pp. 433-444; 445-457.

Backus, G.E., and J.F. Gilbert, 1967, Numerical application of a formalism for geophysical inverse problems, Geophys. J., v. 13, pp. 247-276.

------, 1968, The resolving power of gross earth data, Geophys. J., v. 16, pp. 169-205.

------, 1970, Uniqueness in the inversion of inaccurate gross earth data, Phil. Trans. Roy. Soc. London, A, v. 266, pp. 123-192.

Berezhnaya, L.T., and M.A. Telepin, 1968, Determination of density from gravimetric data, Exploration Geophys., v. 47, pp. 107-113.

Beveridge, G.S.G., and R.S. Schechter, 1970, Optimization: Theory and Practice, 773 pp., McGraw-Hill, New York.

Box, M.J., 1965, A new method of constrained optimization and a comparison with other methods, Computer J., v. 8, pp. 42-52.

------, 1966, A comparison of several current optimization methods, and the use of transformations in constrained problems, Computer J., v. 9 pp. 67-77.

Braile, L.W., G.R. Keller, and W.J. Peebles, 1973, Inversion of gravity profiles for two-dimensional density distributions, paper presented at Utah Inversion Symposium, Salt Lake City, March 13, 1973.

Burg, J.P., 1967, Maximum entropy spectral analysis, presented at 37th Annual Meeting, SEG, Oklahoma City, October 31, 1967.

Cooley, W.W. and P.R. Lohnes, 1971, Multivariate Data Analysis, 364 pp., Wiley, New York.

Cooper, L., and D. Steinberg, 1970, Introduction to Methods of Optimization, 381 pp., W.B. Saunders, Philadelphia.

Corbato, C.E., 1965, A least-squares procedure for gravity interpretation, Geophysics, v. 30, pp. 228-233.

Cordell, L., and R.G. Henderson, 1968, Iterative three-dimensional solution of gravity anomaly data using a digital computer, Geophysics, v. 33, pp. 596-601.

Der, Z.A., and M.Landisman, 1972, Theory for errors, resolution, and separation of unknown variables in inverse problems, with application to the mantle and crust in Southern Africa and Scandinavia, Geophys. J., v. 27, pp. 137-178.

Dunford, N., and J.T. Schwartz, 1958, Linear Operators Part I, Pure and Applied Math., v. 7, 858 pp., Interscience, New York.

Dyrelius, D., and A. Vogel, 1972, Improvement of convergence in iterative gravity interpretation, Geophys. J., v. 27, pp. 195-205.

Fast, J.D., 1968, Entropy, 332 pp., Philips Technical Library, Eindhoven, Holland.

Garland, G.D., 1965, The Earth's Shape and Gravity, 183 pp., Pergamon, London.

Gilbert, F., 1971, Ranking and winnowing gross earth data for inversion and resolution, Geophys. J., v. 23, pp. 125-128.

Grant, F.S., and G.F. West, 1965, Interpretation Theory in Applied Geophysics, 584 pp., McGraw-Hill, New York.

Guin, J.A., 1968, Modification of the Complex method of constrained optimization, Computer J., v. 10, pp. 416-417.

Hoffman, K., and R. Kunze, 1961, Linear Algebra, 332 pp., Prentice-Hall, Englewood Cliffs, N.J.

Jackson, D.D., 1972, Interpretation of inaccurate, insufficient, and inconsistent data, Geophys. J., v. 28, pp. 97-109.

Jackson, D.D., 1973, The EDGEHOG procedure, paper presented at Utah Inversion Symposium, Salt Lake City, March 12, 1973.

Jordan, T.H., and J.N. Franklin, 1971, Optimal solutions to a linear inverse problem in geophysics, Proc. Natl. Acad. Sci. U.S., v. 68, pp. 291-293.

Keilis-Borok, V.I., and T.B. Yanovskaya, 1967, Inverse problems of seismology (structural review), Geophys. J., v. 13, pp. 223-234.

Kittel, C., 1958, Elementary Statistical Physics, 228 pp., Wiley, New York.

Lacoss, R.T., 1971, Data adaptive spectral analysis methods, Geophysics, v. 36, pp. 661-675.

Lathi, B.P., 1968, An Introduction to Random Signals and Communication Theory, 488 pp., International Textbook Co., Scranton, Pa.

MacMillan, W.D., 1930, Theoretical Mechanics: The Theory of the Potential, 469 pp., McGraw-Hill, New York, (reprinted 1958, Dover, New York).

Mottl, J., and L. Mottlova, 1972, Solution of the inverse gravimetric problem with the aid of integer linear programming, Geoexploration, v. 10, pp. 53-62.

Nagy, D., 1966, The gravitational attraction of a right rectangular prism, Geophysics, v. 31, pp. 362-371.

Negi, J.G., and S.C. Garde, 1969, Symmetric matrix method for rapid gravity interpretation, J. Geophys. Res., v. 74, pp. 3804-3807.

Odegard, M.E., and J.W. Berg, 1965, Gravity interpretation using the Fourier integral, Geophysics, v. 30, pp. 424-438.

O'Reilly, D., 1971, Introduction to non-linear function optimization, Informal Documentation, Computing Centre, University of B.C.

Parasnis, D.S., 1962, Principles of Applied Geophysics, 176 pp., Meuthen, London.

Parker, R.L., 1970, The inverse problem of electrical conductivity in the mantle, Geophys. J., v. 22, pp. 121-138.

------, 1972, Inverse theory with grossly inadequate data, Geophys. J., v. 29, pp. 123-138.

------, 1973, A new method of modelling gravity and magnetic anomalies, presented at Utah Inversion Symposium, Salt Lake City, March 13, 1973.

Penrose, R., 1955, A generalized inverse for matrices, Proc. Cambridge Phil. Soc., v. 51, pp. 406-413.

Pierre, D.A., 1969, Optimization Theory with Applications, 612 pp., Wiley, New York.

Press, F., 1968, Earth models obtained by Monte Carlo inversion, J. Geophys. Res., v. 73, pp. 5223-5234.

------, 1970, Earth models consistent with geophysical data, Phys. Earth Planet. Interiors, v. 3, pp. 3-22.

Prigogine, I., G. Nicolis, and A. Babloyantz, 1972, Thermodynamics of evolution, Parts I and II, Physics Today, v. 25, no. 11, pp. 23-28; v. 25, no. 12, pp. 38-44.

Rastrigin, L.A., 1965, Solution of inverse problems by statistical optimization methods, Rev. Geophys., v. 3, pp. 111-114.

Roy, A., 1962, Ambiguity in geophysical interpretation, Geophysics, v. 27, pp. 90-99.

Skeels, D.C., 1947, Ambiguity in gravity interpretation, Geophysics, v. 12, pp. 43-56.

------, 1967, What is residual gravity?, Geophysics, v. 32, pp. 872-876.

Smith, M.L., and J.N. Franklin, 1969, Geophysical applications of generalized inverse theory, J. Geophys. Res., v. 74, pp. 2783-2785.

Sokolnikoff, I.S., and R.M. Redheffer, 1966, Mathematics of Physics and Modern Engineering, 752 pp., McGraw-Hill, New York.

Talwani, M., J.L. Worzel, and M. Landisman, 1959, Rapid gravity computations for two-dimensional bodies with application to the Mendocino submarine fracture zone, J. Geophys. Res., v. 64, pp. 49-59.

Talwani, M., and M. Ewing, 1960, Rapid computation of gravitational attraction of three-dimensional bodies of arbitrary shape, Geophysics, v. 25, pp. 203-225.

Tanner, J.G., 1967, An automated method of gravity interpretation, Geophys. J., v. 13, pp. 339-347.

Ulrych, T.J., 1968, Effect of wavelength filtering on the shape of the residual anomaly, Geophysics, v. 33, pp. 1015-1018.

------, 1972, Maximum entropy power spectrum of truncated sinusoids, J. Geophys. Res., v. 77, pp. 1396-1400.

Wiggins, R.A., 1968, Terrestrial variational tables for the periods and attenuation of the free oscillations, Phys. Earth Planet. Interiors, v. 1, pp. 201-266.

------, 1969, Monte Carlo inversions of body-wave observations, J. Geophys. Res., v. 74, pp. 3171-3181.

Wiggins, R.A., 1972, The general linear inverse problem: implication of surface waves and free oscillations for earth structure, Rev. Geophys. and Space Phys., v. 10, pp. 251-285.

APPENDIX A

Mathematical Concepts

Centroid: The coordinates of the centroid of N points in M-dimensional space are:

$$m_j = \frac{1}{N} \sum_{i=1}^{N} x_{ij} \qquad j = 1,m \qquad \text{(Cooley and Lohnes, 1971, p.30)}$$

Conjugate directions: Any two directions (i.e. unit vectors) $\vec{r}_1$, $\vec{r}_2$ are conjugate for a given matrix A if

$$r_1^T A r_2 = 0 \qquad \text{(Pierre, 1969, p.314)}$$

Convex region: A region is convex if the line segment between any two points of the region is contained entirely within the region.

(Beveridge and Schechter, 1970, p.113)

Distance in an inner product space is given by the norm of $X_1 - X_2$, i.e.

$$D = || X_1 - X_2 || = (X_1 - X_2, X_1 - X_2)^{1/2}$$

where X_1, X_2 denote two points in the space. Depending on the type of inner product defined, this might be

$$D^2 = \int_V (x_1 - x_2)^2 \, dV \qquad \text{or} \qquad D^2 = \sum_{i=1}^{N} (x_{1i} - x_{2i})^2$$

Frechet differential: A function is Frechet differentiable if

$$E(m + dm) = E(m) + (F,dm) + \epsilon(dm)$$

where (F,dm) is an inner product

and $\epsilon(dm)$ approaches zero faster than $||dm||$

F is called the Frechet derivative or Frechet kernel of E.

(Backus and Gilbert, 1967, p. 249)

Hilbert space: a infinite-dimensional linear vector space, over the field of complex numbers, with an associated inner product whose properties are:

a) $(x,x) = 0$ if and only if $x = 0$

b) $(x,x) > 0$

c) $(x+y,z) = (x,z) + (y,z)$

d) $(\alpha x,y) = \alpha(x,y)$

e) $(x,y) = (y,x)^*$ $* = $ complex conjugate

(Dunford and Schwartz, 1958, p.242)

Inner product: A scalar valued function of a pair of vectors (x,y) of the properties shown above. Examples are:

$$(A,B) = \sum_i \sum_j A_{ij} B_{ij}^* \qquad\qquad (f,g) = \int_0^1 f(t)\, g^*(t)\, dt$$

(Hoffman and Kunze, 1961, pp. 221-222)

Norm: The norm on an inner product space is

$$||x|| = (x,x)^{1/2}$$ (Dunford and Schwartz, 1958)

APPENDIX B

Units In Gravity Modelling

Before applying the equations for gravitational attraction of the cells comprising the linear model, they are adapted to allow convenient units for the density and distance parameters. The units to be used are:

$$[g_z] = \text{milligal} = 10^3 \times \text{cm/sec}^2$$

$$[\rho] = \text{gram/cubic centimeter}$$

$$[z], [x] = \text{kilometer}$$

The vertical gravity due to a horizontal cylinder, which we take to approximate the gravity of a prism, is

$$g_z = \frac{(2)\ (\gamma)\ (z_o)\ (\text{mass})}{(x-x_o)^2 + z_o^2} \qquad (1)$$

The gravitational constant is $\gamma = 6.67 \times 10^{-8}$ dyne-cm^2/gm^2

$$= 6.67 \times 10^{-8}\ \text{cm}^3/\text{sec}^2\text{-gm}$$

(mass) here is mass per unit length, equivalent to a horizontal prism dx by dz, of density ρ.

i.e. (mass) = $\rho\,(dx)(dz)$

The appropriate units are

$$(\text{mass}) = \text{gm-km}^2/\text{cm}^3$$

Thus g_z in (1) has units

$$[g_z] = [\gamma]\ (\text{mass})\ [\ \frac{z_o}{(x-x_o)^2 + z_o^2}\ ]$$

$$= \frac{\text{cm}^3}{\text{sec}^2\text{-gm}} \times \frac{\text{gm-km}^2}{\text{cm}^3} \times \frac{1}{\text{km}}$$

$$= \text{km/ sec}^2$$

To transform g_z to milligal, we multiply by 10^8, since 1 km = 10^5 cm and 1 mgal = 10^{-3} cm/sec^2. We are thus using a gravitational constant

$$\gamma = 6.67$$

in calculating the Frechet kernels.

APPENDIX C

Derivations For Backus-Gilbert Inversions

I.   We wish to find a model M which satisfies the observed gravity

data, i.e.

$$g_j (M) = \lambda_j \qquad j = 1,k \qquad (1)$$

and is the "closest" such model to an initial estimate M_G. The model para-

meters are the densities of various rectangular prisms; linearity of g with

density enables us to write

$$g_j(M) = (G_j, M) \qquad (2)$$

where G_j is the Frechet kernel for gravity at the jth station

and (G_j, M) denotes an inner product

In parameter space, the distance of M from M_G is given by

$$||M-M_G||^2 = (M-M_G, M-M_G) = \int_V (\rho-\rho_G)^2 \, dV \qquad (3)$$

where ρ and ρ_G are the densities of the models, and V denotes the subsurface

region containing the models. The gravity effect of the initial model is

$$g_j(M_G) = (G_j, M_G)$$

which is combined with (1) and (2) to give

$$\lambda_j - g_j(M_G) = (G_j, M-M_G) = \int_V G_j(\rho-\rho_G) \, dV \qquad j = 1,K \qquad (4)$$

The problem is then to minimize (3), subject to the constraints (4); which

can be solved using Lagrangian multipliers (Sokolnikoff and Redheffer, 1966,

p.346). The minimum is located by finding a stationary point of

$$F(\rho) = \frac{1}{2} \int_V (\rho - \rho_G)^2 \, dV - \sum_1^K \alpha_j [g_j(M_G) + \int_V G_j(\rho - \rho_G) \, dV - \lambda_j] \quad (5)$$

Taking $\frac{\partial F}{\partial \rho} = 0$, and observing that

$$\frac{\partial}{\partial \rho} \left[\int_V \frac{(\rho - \rho_G)^2}{2} \, dV \right] = \int_V (\rho - \rho_G) \, dV$$

$$\frac{\partial}{\partial \rho} g_j(M_G) = 0$$

$$\frac{\partial}{\partial \rho} \lambda_j = 0$$

$$\frac{\partial}{\partial \rho} \int_V G_j(\rho - \rho_G) \, dV = \int_V G_j \, dV$$

We have

$$\int_V (\rho - \rho_G) \, dV - \sum_1^K \alpha_j \int_V G_j \, dV = 0$$

For the solution to be valid at all points of V, we require

$$\rho = \rho_G + \sum_1^K \alpha_j G_j$$

for all points of V, which is written as

$$M = M_G + \sum_1^K \alpha_j G_j \quad (6)$$

To evaluate the α_j, substitute (6) into (4)

$$\lambda_j - g_j(M_G) = \int_V G_j(\rho - \rho_G) \, dV = \int_V \sum_1^K \alpha_k G_k G_j \, dV \qquad \text{or}$$

$$\lambda_j - g_j(M_G) = \sum_1^K \alpha_k (G_k, G_j) \tag{7}$$

in the inner product notation.

Equation (7) is a linear system which can be solved for α_k by standard matrix methods, since the inner products (G_k, G_j) form a square matrix of dimension K. The steps in the solution are:

a) Compute the Frechet kernels and their inner products

b) Compute gravity of initial model

c) Solve (7) for the Lagrangian multipliers α_k

d) Use the α_k in (6) to find the final model M.

II. Similar systems can be devised to optimize other properties of the model. One possibility is to minimize $||MR||^2$, where R is a spatial weighting factor, which allows us to discriminate against subregions of V in finding a model. In this case the constraints analogous to (4) are simply

$$\lambda_j = g_j(M)$$

and (5) becomes

$$F(\rho) = \frac{1}{2} \int_V \rho^2 R^2 \, dV - \sum_1^K \alpha_j [\int_V G_j \rho \, dV - \lambda_j]$$

Taking $\frac{\partial F}{\partial \rho} = 0$ as before, the solution is

$$\rho = \sum_1^K \frac{\alpha_k G_k}{R^2} \tag{8}$$

Again, we find the α_k by applying the constraints to get

$$\lambda_j = \int_V \frac{G_j \sum_1^K \alpha_k G_k}{R^2} \, dV \qquad \text{or}$$

$$\lambda_j = \sum_1^K \alpha_k \left(\frac{G_k}{R} , \frac{G_j}{R} \right) \tag{9}$$

in the inner product notation. This is also a linear system, which we solve for α_k to use in (8).

III.   The most flexible approach is to combine the methods of I and II, allowing use of an initial model as well as spatial weighting factors. We now want to minimize

$$|| (M - M_G) R ||^2 = \int_V (\rho - \rho_G)^2 \, R^2 \, dV$$

Equation (9) becomes

$$\lambda_j - g_j(M_G) = \sum_1^K \alpha_k \left(\frac{G_j}{R} , \frac{G_k}{R} \right) \tag{10}$$

and the final model is given by

$$\rho = \rho_g + \sum_1^K \frac{\alpha_j G_j}{R^2} \tag{11}$$

Note. All these derivations have written inner products as integrals, e.g.

$$g_j = \int_V G_j \, \rho \, dV$$

For the multi-prism models, the inner products are really summations of the

form

$$g_j = \sum_n \sum_m G_{jnm} \, \rho_{nm}$$

where j denotes surface position

and [n,m] indicates subsurface location of the prism

Thus in applying these results, the integrals are replaced by the appropriate summations. The derivations could be repeated using summations, but this would not change the results.

Notation. M denotes a complete model; i.e. a set of densities.

ρ denotes density as a spatial variable, or density of individual prisms.

APPENDIX D

Numerical Optimization Techniques

Finding a model to fit any geophysical data very often requires

optimization processes. When the data functionals are non-linear, one fre-

quently seeks unique model parameters by minimizing errors of the model

predictions compared to the observed data. If a non-unique class of models

is being considered, a particular model can be selected by optimizing some

property of the model with the constraints that the predictions of the model

agree with the observations (within some limit). The nature of the model,

the number of parameters, and the type of "objective function" to be opti-

mized often make the analytical methods of variational calculus unsuitable.

In these cases, the basic approach to the problem is to seek an optimal point

in parameter space; i.e. the N model parameters are each considered as

coordinates of an N-dimensional space, and the optimum model is then a point

in that space whose location is determined by the optimum value of the

objective function.

Parameter optimization methods have seen some geophysical applica-

tions in recent years. Rastrigin (1965) developed a theoretical procedure

to minimize error between model predictions and observed data, and dis-

cussed some simple methods of "searching" for the optimum point. Al-Chalabi

(1971, 1972) used searches in parameter space to find polygonal models

(following the Talwani procedure) which gave optimum fits to gravity profiles.

The HEDGEHOG and EDGEHOG methods (Jackson, 1973) employ searches to produce

density and velocity models of the upper mantle from seismic data (EDGE-

HOG is a refinement aimed at defining the envelope of all models which fit the data).

A considerable literature has now developed on the subject of numerical optimization. Cooper and Steinberg (1970) gave a good review of basic mathematical concepts, along with descriptions of several commonly used procedures. Box et al (1969) briefly reviewed several methods with a view towards choosing methods for a particular problem. Pierre (1969) described the commonly used techniques, with some discussion of computer application. An excellent book by Beveridge and Schechter (1970) examined the subject in detail, recommending methods proven in practice, and discussing the procedures best suited to particular problems.

In general, numerical optimization methods attempt to locate an optimum in a series of moves starting from a given point. The basis of any method is the means of selecting the direction and length of each move. Methods can be roughly classified using two basic criteria: (1) whether or not constraints on the coordinates (parameters) can be incorporated; and (2) whether or not gradients are used. The usual terminology is that a "direct" search does not employ gradients. The efficiency and speed of search differs between these groups; however the type of problem to be solved may dictate which class of procedure to use. As a general rule, unconstrained gradient methods are fastest. An evaluation of methods falling into each class can be found in the following sections of Beveridge and Schechter:

1) Unconstrained direct search   pp. 363-406

2) Unconstrained gradient search   pp. 407-433

3) Constrained direct search   pp. 448-456

4) Constrained gradient search   pp. 435-448; 457-483

The following brief review follows their descriptions.

Unconstrained optimization is naturally much faster than a con-
strained problem, since motion in parameter space need not be confined to
particular regions.   Direct search methods may either move in prescribed
directions, or use values of the objective function to determine the search
direction.   The basic systematic search method is univariant search, in
which an optimum is found along each coordinate axis from the initial point;
unfortunately this is usually inefficient.   Rosenbrock's method (Beveridge
and Schechter, 1970, p.404) is an effective and reliable adaptation of the
basic idea, allowing acceleration in distance and change of direction.   The
Sequential Simplex method (p.372) determines moves from objective function
values; basically one evaluates the objective function at the vertices of
an n-sided "simplex" in parameter space, and replaces the vertex of worst
function value by reflecting it through the centroid of the figure.

Faster convergence is often possible if gradients of the objec-
tive function can be used.   The simplest application is to move a given
distance in the direction of steepest ascent or descent (i.e. the gradient
direction) in hopes of eventually finding a stationary value of the objective
function.   The method is not usually recommended, since the gradient is
often only a local property which does not "point" to the optimum; in addi-
tion, oscillations about the optimum can result from the fixed distance of

each step. An efficient method which will converge is searching along con-
jugate directions (See Appendix A for definition) until the gradient direction
becomes perpendicular, whereupon new conjugate directions are selected.
Several techniques have been suggested for selecting conjugate directions;
the frequently recommended Davidon-Fletcher-Powell method (Box et al, p.30;
Pierre, p.320; Beveridge and Schechter, p.426) employs the gradient of the
objective function at the initial point.

Constrained optimization is a more difficult task, and a common
approach is to avoid constraints as much as possible. In some cases, this
can be achieved by transformation of variables (Box, 1966). Another method
is to create a new objective function by adding the constraints (multiplied
by a suitably large constant) and then use an unconstrained method (Beveridge
and Schechter, pp.443-448; 477-482). Incorporating constraints as "penalty
functions" in this way keeps the search out of unfeasible regions (where
the constraints are not satisfied and the modified objective function has
a value far from the optimum). The penalty function methods are often im-
practical, since the objective function is distorted near boundaries, and
since the choice of weighting factors to apply to violated constraints may
be critical to the success of the optimization.

Many techniques have been developed to incorporate constraints
directly. In general, all constraints may be considered to be inequalities,
since an equality can be expressed as two inequalities, and since equalities
involving real data usually have some allowable error. The most widely used
methods are probably those of linear programming (Beveridge and Schechter,

pp. 287-322), which deal with problems where all constraints and the object-ive function are linear functions of the parameters; the feasible region then has linear boundaries. Since the objective function is also linear, the optimum must lie on a corner of the feasible region, and efficient matrix methods are available to find this optimum corner. More general problems may be solved with variations of the unconstrained methods. The usually recommended direct method is the Complex method (Box, 1965), which stems from the Sequential Simplex method. Details of the method are given in Appendix E.

Gradient methods usually require linearization of constraints to be most effective, and usually incorporate constraints into the choice of search direction to avoid leaving the feasible region. The hemstitching technique (Beveridge and Schechter, p.456) allows any method of choosing the search direction, but follows the gradient of a constraint to move back into the feasible region whenever any constraint is violated; unfortunately this often means that the search is not moving towards the optimum point. Rosen's gradient projection (Beveridge and Schechter, p.469), or the method of riding constraints (Box et al, p.42) always use the constraints in choosing the search direction to ensure that the search stays in the feasible region. Linear constraints can be added to the Davidon-Fletcher-Powell method of choosing conjugate directions (Box et al, p.47), and thus this efficient method can be applied to some constrained problems. Beveridge and Schechter suggest that most of these methods have the basic problems of steepest ascent searches, and recommend the Complex method for most non-linear constrained problems, particularly if the optimum is expected near a boundary of the region.

APPENDIX E

The Complex Method

The Complex method of numerical optimization (Box, 1965) can be

applied to many different problems, since it does not require any special

type of objective function. The search procedure is similar to the Sequen-

tial Simplex method (see Appendix D), but incorporates constraints on the

parameters of the objective function. The only problem in implementation

is that an initial feasible point (i.e. one which satisfies all the con-

straints) is required before the search begins.

The allowable constraints are bounds on all the model parameters,

$$A_i \leqslant x_i \leqslant B_i \qquad i = 1,N \qquad (1)$$

plus implicit constraints of the form

$$y_j \leqslant C_j \qquad j = 1,M \qquad (2)$$

where y_j are functions of the x_i. With a known initial point, the other

vertices of the "complex" are found as follows: the coordinates x_i of each

point are generated randomly in the intervals (A_i,B_i); the quantities y_j are

calculated for the point; if any of the implicit constraints are not satis-

fied, the point is moved halfway towards the centroid of feasible points as

many times as are necessary to make the trial point satisfy all the con-

straints. This method ensures that other feasible points can be found, so

long as the region defined by the constraints is convex (see Appendix A).

The process is repeated until a complex of k vertices (k>N+1) is established

(each vertex is a point in the "feasible" region of the parameter space,

i.e. the region where all the constraints are satisfied).

Once the complex has been set, the objective function is evaluated at each vertex, and the vertex of worst value (smallest for maximization; largest for minimization) is replaced by over-reflection through the centroid of remaining points. The coordinates of the new vertex are

$$X'_{i,R} = \alpha(X_{i,R} - C_i) + C_i \qquad (3)$$

where $X_{i,R}$ = coordinates of worst vertex

$X'_{i,R}$ = coordinates of replacement

C_i = coordinates of the centroid of all other vertices, given by

$$C_i = \frac{1}{K-1} (\sum_{j=1}^{K} X_{i,j} - X_{i,R}) \qquad (4)$$

and α is an expansion parameter (Box suggests $\alpha \approx 1.3$)

Of course, the replacement point must satisfy all the constraints (equations (1) and (2)). If any coordinate $X'_{i,R}$ does not lie in the required interval (A_i, B_i), it is given a value just inside the appropriate bound. If any implicit constraint (equation 2) is violated, the trial point is moved halfway towards the centroid of other points and tested again; the new point is then

$$X''_{i,R} = 0.5 (X'_{i,R} + C_i) \qquad (5)$$

Once an acceptable new point is found, the rejection process is repeated with the current worst point. The search could stall if the replacement point still has the worst function value. To avoid this problem, Box

suggested moving such a point halfway toward the centroid, rather than reflecting it back again.

Guin (1968) suggested some modifications to the method, which allow it to be used in non-convex regions. In a non-convex region, the centroid may eventually fall outside the region, making it impossible to find new feasible points by moving towards the centroid. In this eventuality, Guin suggested creating a new complex using the "best" point as the initial point, and creating other points by random generation in the interval between the best point and the old centroid. The coordinates of a new point are then

$$X_{i,j} = X_{i,o} + R (C_i - X_{i,o}) \tag{6}$$

    where $X_{i,o}$ are the coordinates of the best point

        C_i are coordinates of the old centroid

        R is a random number $(0 < R < 1)$

Each point is tested for feasibility and moved towards the current centroid if necessary. Guin's other ideas were to reject the second worst point if one point is continually the worst, and to move a trial point halfway towards the centroid if a bound on a variable (i.e. coordinate) is exceeded.

An additional feature has been implemented by the University of B.C. Computing Centre. They suggest periodically restarting the complex (following Box's method) to accelerate searching when far from the optimum

(O'Reilly, 1971); a new complex is created from the best point after a specified number of iterations, but not after a maximum number has been passed.

The actual search procedure used for the minimum entropy problem follows Box's basic method, incorporating some of the other suggestions and some new variations. Restarting is optional after a specified number of iterations; the new complex may be produced by random number generation in the complete interval (A_i, B_i), or in the region near the best point and the old centroid. In the latter case, Guin's method has been slightly altered by using a random number (R in equation (6)) evenly distributed between -1 and +1, thus the coordinates of a new point can fall on both sides of the best point relative to the old centroid. Guin's suggestion for generating a new complex if the centroid becomes an unfeasible point was adopted. When one point is consistently the worst, a new complex is generated from the current best best point, since this problem was found to be an indication that the search was not progressing very well. This strategy proved more successful than Box's suggestion, since repeated moves toward the centroid can lead to apparent convergence of the search, if the centroid itself has the worst function value.

When the optimum has been reached, all the vertices of the complex should approach the centroid; hence the convergence test is to evaluate the objective function at the centroid, and stop the search when several successive evaluations agree within a specified limit. In addition, a specified maximum number of iterations will stop searching, to avoid using excessive computer time when progress is slow.

APPENDIX F

Computer Program

The required inputs are as follows.

M1, M2, N1, N2 define the locations of blocks to be used in the model.

JA = 1 defines the first gravity station (M is measured from JA).

JB = number of data in the profile.

DX = DZ = station spacing = cell dimension.

WT, WT2, WT3 are weighting factors to apply to each cell in the model.

REG(N,M) an indicator (0.0, 1.0, 2.0, 3.0) of which weighting factor to apply (1.0, WT, WT2, WT3).

RHO(N,M) = cell densities for the initial model.

GZO(J) = the gravity profile.

Other routines mentioned.

FSLE: a UBC Computing Centre routine which solves

[PROD(J,K)] [Y(J)] = [B(K)].

HIST: an optional line-printer plot of the data.

In SMOOTH, C is the desired increment of density to be displayed.

```
C    "WEIGHT"
C **
C  A PROGRAM TO COMPUTE MODELS FROM WEIGHTED REGIONS OF THE
C  SUBSURFACE GRID
      REAL Z(10),G(30,10,30),PROD(30,30),GZO(30),E(30),DENS(10,30),
     1X(30),GZM(30),T(30,30),RR(10,30),Y(30),MASS,REG(10,30),
     2RHO(10,30),B(30),GZ(30),YNAM(100),XNAM(100)
      INTEGER IPERM(100)
C  EACH CELL HAS AN ASSIGNED WEIGHT OF "WT" OR 1.0,DEPENDING ON
C  THE SPECIFIED VALUE OF REG(N,M):  THE MODEL IS FOUND BY MINIMIZING
C  THE SUM OF (|DENS-RHO|*RR) SQUARED
      READ(5,3) M1,M2,N1,N2,JA,JB,DX,DZ,WT,WT2,WT3
      DO 5 I=1,30
      Z(I)=(I-.5)*DZ
5     X(I)=I*DX
3     FORMAT(6I5,5F10.3)
C  THE INITIAL MODEL AND REGIONS TO BE WEIGHTED ARE GIVEN
      READ(5,4)  ((REG(N,M),N=1,10),M=M1,M2)
4     FORMAT(10F5.2)
      READ(5,4)  ((RHO(N,M),N=1,10),M=M1,M2)
C  DISPLAY THE INITIAL MODEL
      WRITE(6,16)  (Z(N),N=N1,N2)
16    FORMAT(//1X,'INITIAL MODEL',/,1X,' X (KM) / Z= ',10F8.2)
      WRITE(6,31)
      DO 17 M=M1,M2
17    WRITE(6,40) X(M),(RHO(N,M),N=N1,N2)
C **
C  THE FRECHET KERNELS FOR GZ ARE COMPUTED; "C" CORRECTS THE CYLINDER
C  EXPRESSION TO THAT OF A RECTANGULAR PRISM OF EQUAL MASS
      DO 10 J=JA,JB
      DO 10 M=M1,M2
      DO 10 N=N1,N2
      IF(J.EQ.M.AND.N.EQ.1)C=.86601
      IF(IABS(J-M).EQ.1.AND.N.EQ.1) C=.98145
      IF(J.EQ.M.AND.N.EQ.2) C=0.99676
      IF(IABS(J-M).GT.1.OR.N.GT.1) C=1.0
```

```
      RR (N,M)=1.0
      IF(REG(N,M).EQ.1.0)  RR(N,M)=WT
      IF(REG(N,M).EQ.2.0)  RR(N,M)=WT2
      IF(REG(N,M).EQ.3.0)  RR(N,M)=WT3
10    G(J,N,M)=2.0*C*Z(N)*DX*DZ*6.67/((X(J)-X(M))**2+Z(N)*Z(N))
C  THE WEIGHTED REGIONS ARE DISPLAYED
      WRITE(6,27)  (Z(N),N=N1,N2)
27    FORMAT(//1X,'WEIGHTED REGIONS',/,1X,
     1' X (KM) / Z= ',10F8.2)
      WRITE(6,31)
      DO 28 M=M1,M2
28    WRITE(6,40)  X(M),(REG(N,M),N=N1,N2)
      WRITE(6,29)  WT,WT2,WT3
29    FORMAT(/1X,'THE WEIGHTING FACTOR IN CELLS MARKED 1.0 IS',F9.1,
     2/,1X,'THE WEIGHTING FACTOR IN CELLS MARKED 2.0 IS',F9.1,
     3/,1X,'THE WEIGHTING FACTOR IN CELLS MARKED 3.0 IS',F9.1,
     1/,1X,'OTHER REGIONS HAVE UNIT WEIGHT IN THE MINIMIZATION')
C ***
C  THE INNER PRODUCTS OF THE FRECHET KERNELS ARE GENERATED
      DO 15 J=JA,JB
      DO 15 K=JA,JB
      PROD(J,K)=0.0
      DO 15 M=M1,M2
      DO 15 N=N1,N2
15    PROD(J,K)=PROD(J,K)+G(J,N,M)*G(K,N,M)/RR(N,M)
C ***
C  THE LAGRANGE MULTIPLIERS ARE FOUND BY SOLVING THE MATRIX PROD;
C  "FSLE" IS A COMPUTING CENTRE ROUTINE FOR SIMULTANEOUS EQUATIONS
      READ(5,20)  (GZO(J),J=JA,JB)
20    FORMAT(6F12.3)
      WRITE(6,18)
18    FORMAT(//1X,'  X  GZ(MODEL)   GZ(REAL)   DIFFERENCE'/)
      DO 22 J=JA,JB
      GZ(J)=0.0
      DO 21 M=M1,M2
      DO 21 N=N1,N2
21    GZ(J)=GZ(J)+G(J,N,M)*RHO(N,M)
      B(J)=GZO(J)-GZ(J)
22    WRITE(6,23)  J,GZ(J),GZO(J),B(J)
23    FORMAT(1X,I4,3F10.4)
```

```
      JLN=JB-JA+1
      LENA=30
      LENBX=30
      LENT=30
      NSOL=1
      CALL FSLE(JLN,LENA,PROD,NSOL,LENBX,B,Y,IPERM,LENT,T,DET,JEXP)
C ***
C  THE FINAL MODEL IS COMPUTED USING THE LAGRANGE MULTIPLIERS Y
C ***
      DO 26 M=M1,M2
      DO 26 N=N1,N2
      DENS(N,M)=0.0
      DO 25 J=JA,JB
25    DENS(N,M)=DENS(N,M)+Y(J)*G(J,N,M)
26    DENS(N,M)=DENS(N,M)/RR(N,M)+RHO(N,M)
      WRITE (6,30) (Z(N),N=N1,N2)
30    FORMAT (1X,//,1X,'COMPUTED DENSITIES',//,1X,' X (KM) / Z= ',
     110F8.2)
      WRITE (6,31)
31    FORMAT(1X,'................................')
      DO 35 M=M1,M2
35    WRITE (6,40) X(M),(DENS(N,M),N=N1,N2)
40    FORMAT (1X,F8.2,'  :   ',10F8.3)
C ***
C  THE GRAVITY EFFECT AND MASS OF THE FINAL MODEL ARE COMPUTED
C  AND DISPLAYED
      WRITE (6,42)
42    FORMAT (1X,//,1X,'OBSERVED GRAVITY - MODEL GRAVITY - ERROR'//)
      DO 50 J=JA,JB
      GZM(J)=0.0
      MASS=0.0
      DO 45 M=M1,M2
      DO 45 N=N1,N2
      MASS=MASS+DENS(N,M)
45    GZM(J)=GZM(J)+DENS(N,M)*G(J,N,M)
      E(J)=GZO(J)-GZM(J)
50    WRITE(6,55) J,GZO(J),GZM(J),E(J)
55    FORMAT (1X,I5,2F11.4,F10.4)
```

```
          WRITE (6,60) MASS
60        FORMAT (1X,///,1X,'TOTAL MASS IS   ',F10.4//)
C  PLOT THE GRAVITY PROFILE
          READ (6,65) XMN,XMX
65        FORMAT (2F10.4)
          READ (5,70)  (YNAM(I),I=1,80)
          READ (5,70)  (XNAM(I),I=1,80)
70        FORMAT (80A1)
          CALL HIST (GZO,JLN,DX,YNAM,XNAM,XMN,XMX,1)
C  COMPUTE AN APPROXIMATE MODEL
          CALL SMOOTH (DENS,G,M1,N1,M2,N2,X,Z,MASS,JA,JB,GZO)
          STOP
          END



          SUBROUTINE SMOOTH (DENS,G,M1,N1,M2,N2,X,Z,MASS,JA,JB,GZO)
          REAL ADENS (10,30),GZO (30),GA (30),MASS,AMASS,ER (30),C,X (30),
         1Z (30),DENS (10,30),G (30,10,30)
9         READ  (5,10) C
10        FORMAT  (F10.4)
          IF  (C.EQ.0.0) GO TO 80
12        DO  13 M=M1,M2
          DO  13 N=N1,N2
          ADENS (N,M) =C*FLOAT (IFIX ((DENS (N,M) +0.5*C) /C))
          IF (ADENS (N,M).LE.0.0)  ADENS (N,M) =0.0
13        CONTINUE
C   NOW COMPUTE AND COMPARE GRAVITIES
          DO  15 J=JA,JB
          GA (J) =0.0
          AMASS=0.0
          DO  14 M=M1,M2
          DO  14 N=N1,N2
          GA (J) =GA (J) +ADENS (N,M) *G (J,N,M)
14        AMASS=AMASS+ADENS (N,M)
15        ER (J) =GZO (J) -GA (J)
```

```
      WRITE (6,30) (Z(N),N=N1,N2)
30    FORMAT(//1X,'APPROXIMATE DENSITIES',//,1X,
     1'X  (KM) / Z=',10F8.2)
      WRITE (6,33)
33    FORMAT(1X,'...............................')
      DO 35 M=M1,M2
35    WRITE (6,37) X(M),(ADENS(N,M),N=N1,N2)
37    FORMAT(1X,F8.2,' : ',10F8.2)
      WRITE (6,42)
42    FORMAT(//1X,'EXACT GRAVITY - APPROX GRAVITY - ERROR'/)
      DO 50 J=JA,JB
50    WRITE (6,55) J,GZO(J),GA(J),ER(J)
55    FORMAT (1X,I5,2F11.4,F10.4)
      WRITE (6,60) MASS,AMASS
60    FORMAT (1X,///,'TRUE MASS IS     ',F10.4,/,1X,
     1'APPROX. MASS IS  ',F10.4)
      GO TO 9
80    RETURN
      END
```